Calhoun
Institutional Archive of the Naval Postgraduate School

Calhoun: The NPS Institutional Archive

DSpace Repository

Theses and Dissertations | 1. Thesis and Dissertation Collection, all items

1964

Power amplification with gate turn-off controlled rectifiers

Camacho, Richard G.

http://hdl.handle.net/10945/12859

This publication is a work of the U.S. Government as defined in Title 17, United States Code, Section 101. Copyright protection is not available for this work in the United States.

Downloaded from NPS Archive: Calhoun

DUDLEY
KNOX
LIBRARY

Calhoun is the Naval Postgraduate School's public access digital repository for research materials and institutional publications created by the NPS community. Calhoun is named for Professor of Mathematics Guy K. Calhoun, NPS's first appointed -- and published -- scholarly author.

Dudley Knox Library / Naval Postgraduate School
411 Dyer Road / 1 University Circle
Monterey, California USA 93943

http://www.nps.edu/library

NPS ARCHIVE
1964
CAMACHO, R.

POWER AMPLIFICATION WITH GATE TURN-OFF CONTROLLED RECTIFIERS

RICHARD G. CAMACHO

Library
U. S. Naval Postgraduate School
Monterey, California

9

POWER AMPLIFICATION WITH GATE TURN-OFF CONTROLLED RECTIFIERS

* * * * *

Richard G. Camacho

POWER AMPLIFICATION WITH
GATE TURN-OFF CONTROLLED RECTIFIERS

by

Richard G. Camacho

Lieutenant, United States Navy

Submitted in partial fulfillment of
the requirements for the degree of

MASTER OF SCIENCE
IN
ELECTRICAL ENGINEERING

United States Naval Postgraduate School
Monterey, California

1 9 6 4

PS ARCHIVE
964
AMACHO.R.

Library
U. S. Naval Postgraduate School
Monterey, California

POWER AMPLIFICATION WITH
GATE TURN-OFF CONTROLLED RECTIFIERS

by

Richard G. Camacho

This work is accepted as fulfilling
the thesis requirements for the degree of

MASTER OF SCIENCE

IN

ELECTRICAL ENGINEERING

from the

United States Naval Postgraduate School

ABSTRACT

With ever larger amounts of power being required by present day active sonars, studies are being made towards improving the efficiency of the power train. A gain in efficiency is possible if non-linear switching type amplifiers are used in lieu of the linear amplifiers presently used. Due to its high switching efficiency, fast switching, and ability to be turned on or off by gate signals, the Gate Turn-off Controlled Rectifier was investigated for possible application in an amplifier circuit.

The circuit examined readily met the required criteria, however, the real value of this study lies in the method of predicting transient performance. Use of the derived equivalent circuit, and an analog computer model based on transfer functions (E_L/E and i_1/E), provide analytical solutions that can be arrived at more readily than by other methods.

TABLE OF CONTENTS

Page

CHAPTER I

The Gate Turn-off Controlled Rectifier

I.1 Introduction 1

I.2 Turn-On Criterion 2

I.3 Gate Characteristics 7

CHAPTER II

An Analysis of the Basic Power Amplifier

II.1 Introduction 14

II.2 Operation of the Ideal Circuit 16

II.3 Analysis of the Experimental Circuit 21

II.4 Experimental Results for the Basic Power Amplifier 24

II.5 Discussion of Results 33

CHAPTER III

The Power Amplifier with a Transducer Load

III.1 Introduction 35

III.2 Analysis of Transducer Loading 38

III.3 Discussion of Analytical Results 44

III.4 Experimental Results 58

III.5 Conclusions Based on Experimental Results 68

BIBLIOGRAPHY 71

LIST OF ILLUSTRATIONS

Figure		Page
I.1	Voltage-current Operation Characteristics	2
I.2A	Schematic of GTCR	3
I.2B	Two Transister Analog of GTCR	3
I.3	Plot of Emitter Current, I_E vs. α	4
I.4	Typical Gate Characteristics of the WX241W	10
I.5	Gate Characteristics	11
I.6	Typical Turn-Off Gain	12
I.7	Pulse Gate Drive Turn-Off Characteristics	13
II.1	Basic Amplifier	15
II.2	Amplifier Equivalent Circuit	20
II.3	Equivalent Circuit with R + jwL Loading	21
II.4	Laboratory Setup of Basic Amplifier	24
II.5	Analog Circuit for Solution of Amplifier Current	28
II.6	Analog Circuit for Solution of Output Voltage	29
II.7	Predicted Wave Shape for i_1	30
II.8	Predicted Wave Shape for E_L	30
II.9	Observed i_1	32
II.10	Observed E_L	32
II.11	Observed Voltage Drop Across GTCR	32a
III.1	Equivalent Transducer Load	36
III.2	Equivalent Circuit with Transducer Load	38
III.3	Analog Circuit for Amplifier Current	41
III.4	Analog Circuit for Output Voltage	43

List of Illustrations Cont'd

Figure		Page
III.5	i_1 and E_L for C = 0.0021	45
III.6	i_1 and E_L for C = 0.0042	46
III.7	i_1 and E_L for C = 0.00612	47
III.8	i_1 and E_L for C = 0.0082	48
III.9	i_1 and I_L for C = 0.011	49
III.10	i_1 and E_L for C = 0.016	50
III.11	i_1 and E_L for C = 0.0212	51
III.12	i_1 and E_L for L = 9/8 L_1	53
III.13	i_1 and E_L for L - 5/4 L_1	54
III.14	i_1 and E_L for L = 3/2 L_1	55
III.15	i_1 and E_L for L = 2 L_1	56
III.16	i_1 and E_L for L = 6 L_1	57
III.17	Mpt vs ξ	59
III.18	$w_n t_p$ vs ξ	60
III.19	E_L observed,C = .0021	61
III.20	E_L observed,C = .0042	62
III.21	E_L observed, C = .00612	63
III.22	E_L observed, C = .0082	64
III.23	E_L observed, C = .011	65
III.24	E_L observed, C = .016	66
III.25	E_L observed, C = .021	67
A-1	Four Layer Diode Characteristics	73
A-2	Analog Circuit for i_1	76
A-3	Analog Circuit for E_L	81

CHAPTER ONE

THE GATE TURN-OFF CONTROLLED RECTIFIER

I.1 Introduction.

The Gate Turn-off Controlled Rectifier, GTCR, is a three terminal, p-n-p-n silicon structure very similar to the Silicon Controlled Rectifier, SCR. It differs from the SCR in that conduction through the device can be stopped by the application of negative pulses to the gate terminal.

The GTCR enjoys the following advantages which the SCR has over other switching devices: [1]

a. A high switching efficiency.

b. High surge current ratings.

c. Large power gain.

d. Pulse turn on.

e. Extremely fast switching times.

The SCR's were found to be limited in switching capabilities, since the turn-off required either a drop in current below the rated holding current, or the application of a voltage of opposite polarity across the device, so that the operating point is moved into the blocking state.

The typical operating characteristic of both devices is shown in Figure I-1. Note that by applying the gate current, the Forward Breakover Voltage is moved to the left.

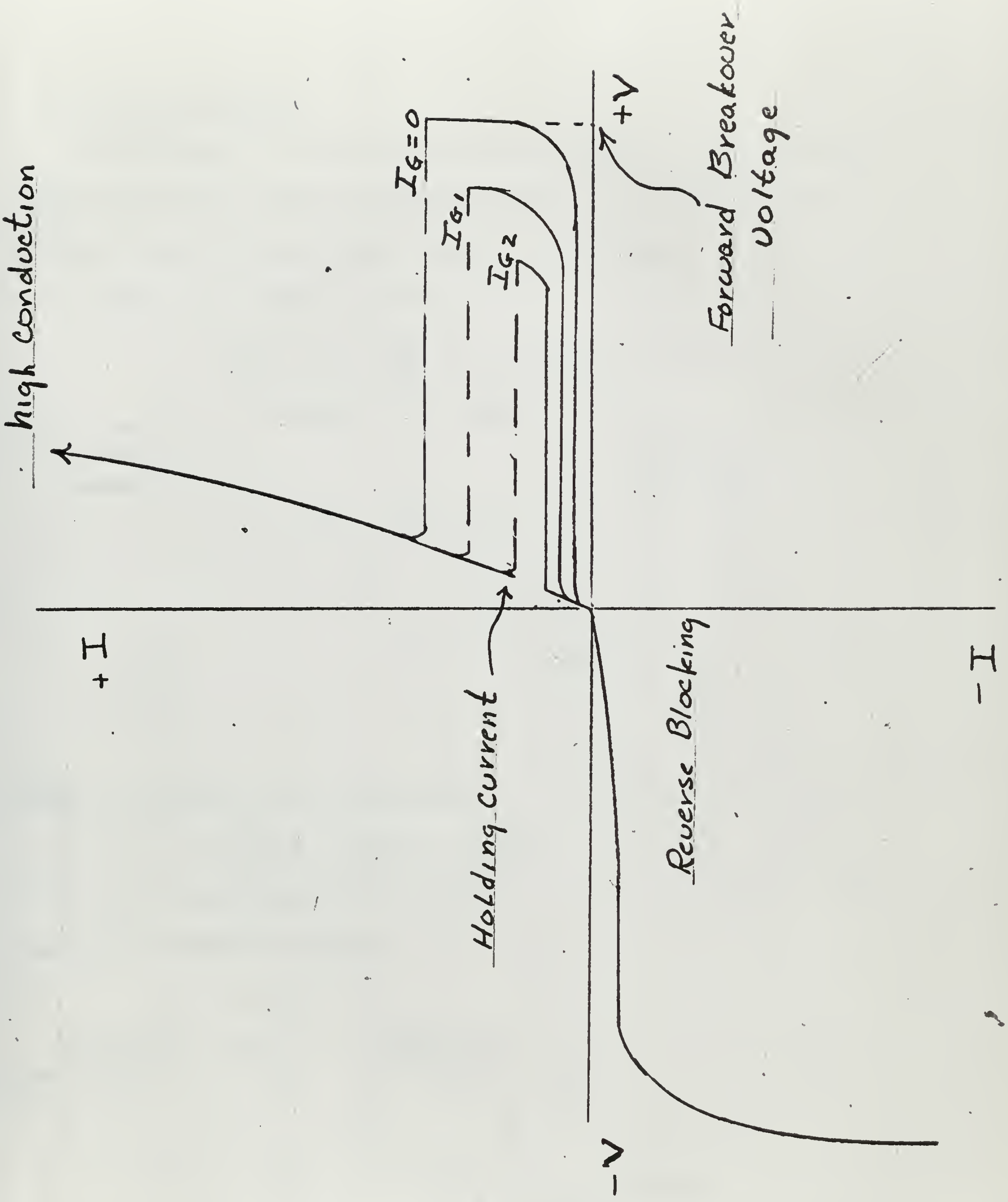
high conduction
I_G=0
I_G1
I_G2
+V
Forward Breakover Voltage
+I
-I
-V
Holding Current
Reverse Blocking

Fig. I-1

I.2 Turn-On Criterion.

In examining the turn-on criterion of the p-n-p-n device we will employ the widely used two transistor analog. [3] Figures I-2A and I-2B show how we can pictorially represent our analog.

Figure I-2A Schematic of GTCR

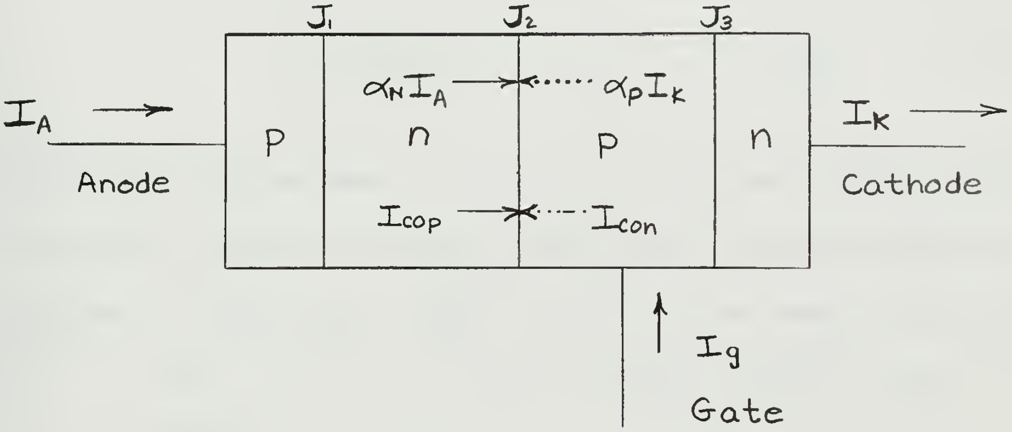

where J_1, J_2 and J_3 are the junctions

...... represents electron current

——— represents hole current

Fig. I-2B 2 Transistor Analog

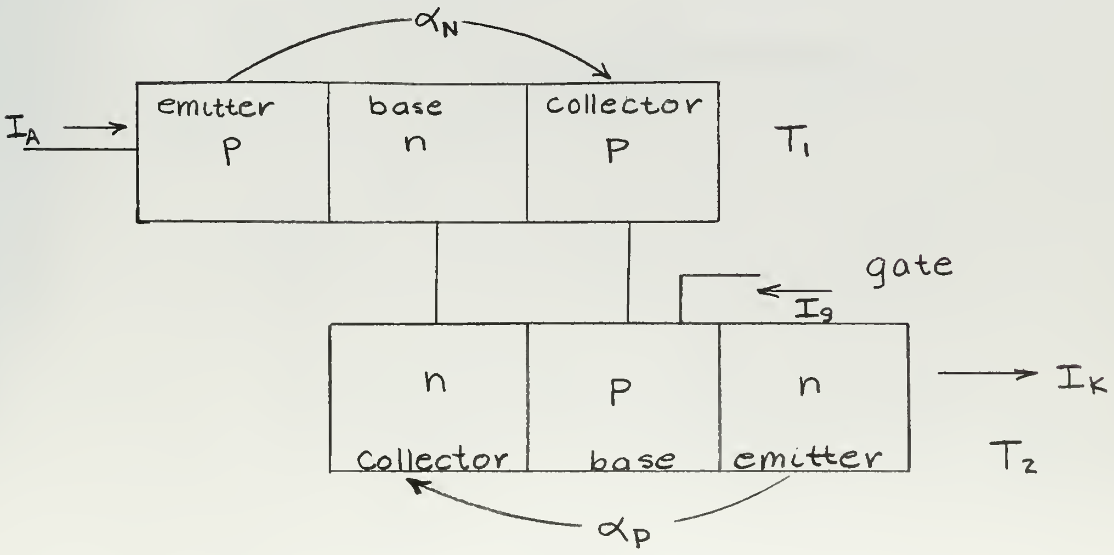

We can define the DC alphas in the usual manner as the ratio of collector current resulting from the emitter current, to the emitter current. Thus in general the total current collected will be:

$$I_c = \alpha I_E + I_{co}$$

where I_{co} is the amount of thermally generated current collected. The small signal α's can then be defined as:

$$\alpha_o = \frac{dI_c}{dI_E} = \alpha + I_E \frac{d\alpha}{dI_E}$$

From Figure I-2A we see that if $I_k = I_a + I_g$ the current through Junction 2 must be I_a which is the sum of the hole, electron, thermal, and displacement current, $I_{dis} = \frac{CdV}{dt}$, where C = the capacitance of J_2

(1) $$I_a = \alpha_N I_a + \alpha_p I_k + I_{co} + I_{dis}$$

since

(2) $$I_k = I_a + I_g$$

$$\therefore \quad I_a = \frac{\alpha_p I_g + I_{co} + I_{dis}}{1 - \alpha_N - \alpha_p}$$

Before discussing the results of this expression let us examine Figure I-3 which shows the general relationship between emitter current I_e and the small signal α's .

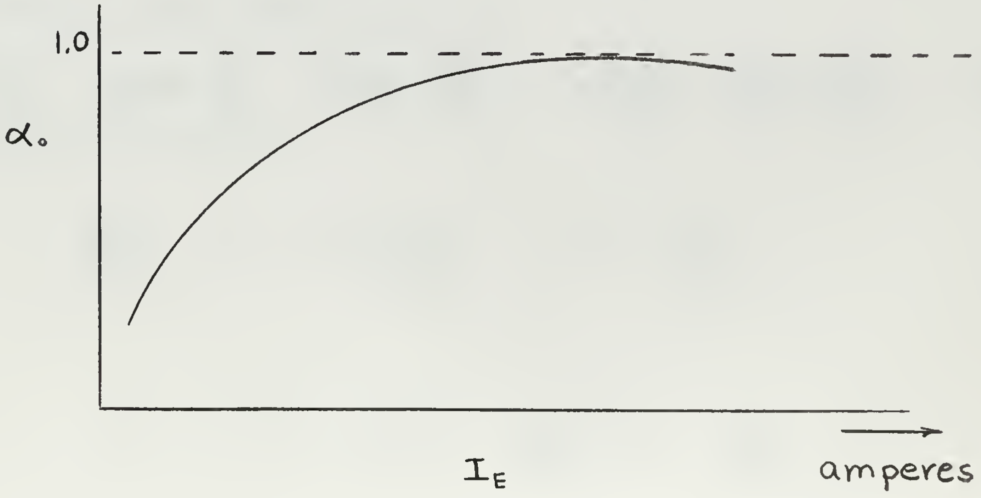

Fig. 3

We can see that the small signal α's increase monotonically with emitter current. We desire now an expression for $\frac{\Delta I_a}{\Delta I_g}$ to see what the small signal requirements are for $\frac{\Delta I_a}{\Delta I_g} \rightarrow \infty$ which is the criteria for switching on.

$\frac{\Delta I_a}{\Delta I_g} \rightarrow \infty$ implies that I_g may $\rightarrow 0$ without affecting I_a. To get the desired relationship, differentiate (1) with respect to I_g.

$$\frac{dI_a}{dI_g} = \alpha_N \frac{dI_a}{dI_g} + I_a \frac{d\alpha_N}{dI_g} + \alpha_p \frac{dI_k}{dI_g} + I_k \frac{d\alpha_p}{dI_g} \tag{3}$$

but as previously shown

$$\frac{d\alpha_N}{dI_a} = \frac{\alpha_{no}}{I_a} - \frac{\alpha_N}{I_a}$$

$$\frac{d\alpha_p}{dI_k} = \frac{\alpha_{po}}{I_k} - \frac{\alpha_p}{I_k}$$

Where α_{no} and α_{po} are the small signal alphas.

We can furthermore simplify to get:

$$\frac{d\alpha_N}{dI_g} = \frac{d\alpha_N}{dI_a} \cdot \frac{dI_a}{dI_g} = \frac{\alpha_{no}}{I_a} \frac{dI_a}{dI_g} - \frac{\alpha_N}{I_a} \frac{dI_a}{dI_g}$$

and

$$\frac{d\alpha_p}{dI_g} = \frac{\alpha_{po}}{I_k} \frac{dI_k}{dI_g} - \frac{\alpha_p}{I_k} \frac{dI_k}{dI_g}$$

Now substitute these results into (3),

$$\frac{dI_a}{dI_g} = \alpha_N \frac{dI_a}{dI_g} + \frac{I_a \alpha_{no}}{I_a} \frac{dI_a}{dI_g} - \frac{I_a \alpha_N}{I_a} \frac{dI_a}{dI_g} + \alpha_p \frac{dI_k}{dI_g} + \frac{I_k \alpha_{po}}{I_k} \frac{dI_k}{dI_g} - \frac{I_k \alpha_p}{I_k} \frac{dI_k}{dI_g}$$

which reduces as follows:

$$\frac{dI_a}{dI_g} = \alpha_{no} \frac{dI_a}{dI_g} + \alpha_{po} \frac{dI_k}{dI_g}$$

since

$$I_k = I_a + I_g, \quad \frac{dI_k}{dI_g} = \frac{dI_a}{dI_g} + 1$$

hence, $\frac{dI_a}{dI_g} = \frac{\alpha_{po}}{1 - \alpha_{po} - \alpha_{no}}$

We are now in a position to form some conclusion regarding switching. For $\alpha_{no} + \alpha_{po} = 1$ we note that $\frac{dI_a}{dI_g} \longrightarrow \infty$. This then is our turn-on requirement, which as we see from Figure I-3 is brought about by α_{po} and α_{no} increasing steadily as their respective emitter currents increase.

Similarly we note that at turn-off, when current is pulled out of the gate, α_P decreases first, then α_N decreases and from equation (2) we see that $I_a \approx I_{co} + I_{dis} - \alpha_P I_g$ which is the very small leakage current.

In the conducting state all three junctions are forward biased and saturated with carriers. Unlike the SCR which requires an additional incremental time to allow for the diffusion of the carriers from the center junction after turnoff, the GTCR is completely turned off when the carriers are removed due to the negative gate pulse. Hence the GTCR is capable of much higher frequency operations.

It becomes apparent then that the function of the amplitude of the gate current is to control the variables α_N and α_P. If I_{co} and I_{dis} are negligible then $\frac{I_a}{I_g} \approx \frac{\alpha_P}{1 - \alpha_P - \alpha_N}$.

As previously discussed for turn-on, we desire to have the gate current such that the emitter currents will cause $\alpha_N + \alpha_P = 1$. Further, for high turn-off gains we would desire $(\alpha_P + \alpha_N) \rightarrow 1$, $\alpha_P > \alpha_N$. At present turn-off gains on the order of 10-20 are possible.

I.3 Gate Characteristics.

There are two means of turning on the GTCR, by exceeding the forward breakover voltage, and by gate currents. Since switching by gate current is the more practical means, we will examine only this method.

The Gate Turn-on and Turn-off characteristics for the Westinghouse WX 241W GTCR are shown in Figures I-4, 5, 6 and 7. [1] These characteristics are considerably affected by:

(a) the gate pulse
   1. magnitude
   2. width

(b) the load

(c) the temperature of the junctions

In addition the turn-off characteristics are affected by the anode current to be turned off.

In Figure I-4 we see the switching locus with I_a as a parameter and gate voltage V_g, and gate current I_g, the variables. These curves were constructed for $R_l = 50$ ohms and $T_j = 125°C$. If we start at $I_a = I_g = V_g = 0$ and move along the $I_a = 0$ curve in the direction of increasing I_g and V_g, we arrive at the turn-on point at which the curve becomes discontinuous and shifts to the curve of the applicable anode current.

Similarly, if we desire to turn the device off we can follow the curve for the operating anode current down to the point marked turn-off, at which we read the required turn-off gate voltage and current. We can readily observe the effects on turn-off requirements for different anode currents from this figure.

In Figure I-5 are plotted the maximum gate power curves showing the rated DC and peak gate power. To gate the device, we must operate below these curves, and above the shaded areas which represent the turn-on and

turn-off boundaries. The advantage of pulse gate drive is that higher currents and terminal voltages may be used without exceeding the power rating of the device. This can be shown by considering the switching efficiency:

$$\text{if, } A_p = \frac{\text{Power out}}{\text{Power in}} = \text{the power gain}$$

$$\text{and} \quad \eta_{\text{switching}} = \frac{\text{Power out}}{\text{Power out} + \text{losses}} = \text{efficiency}$$

and since the power input to the gate does not contribute power to the load, but is all lost

$$\text{power input} = \text{losses} = \frac{\text{P out}}{A_p}$$

the efficiency is then

$$\eta_{\text{switching}} = \frac{\text{P out}}{\text{P out}(1 + 1/A_p)} = \frac{1}{1 + \frac{1}{A_p}}$$

For bistable switching as we have with the GTCR, the time base of the input differs from that of the output, thus the gain A_p must be corrected by the factor $\frac{T_1}{t}$ where:

T_1 = the conduction interval

and t = the gate interval (pulse width)

thus,

$$\eta_{s\ \text{GTCR}} = \frac{1}{1 + \frac{1}{A_p\left(\frac{T_1}{t}\right)}}$$

thus for a T_1 = .50 millisec and a gate pulse width of 10 μsec we have increased the effective gain by a factor of 50.0 and reduced the amount of power to be dissipated in the device.

The variation of the turn-off gains with anode currents for two values of junction temperature are shown in Figure I-6. On examining these curves, we note that the gains decrease with increasing temperature, which can be attributed mainly to the increase in the thermal

currents.

From Figure I-7, we can get an idea about the order of the switching time and power controlled. For the circuit shown in the Figure we observe that 1000 watts can be switched in 5 micro seconds with a source voltage of 500 volts, anode current of 2 amperes, and junction temperature of 80°C.

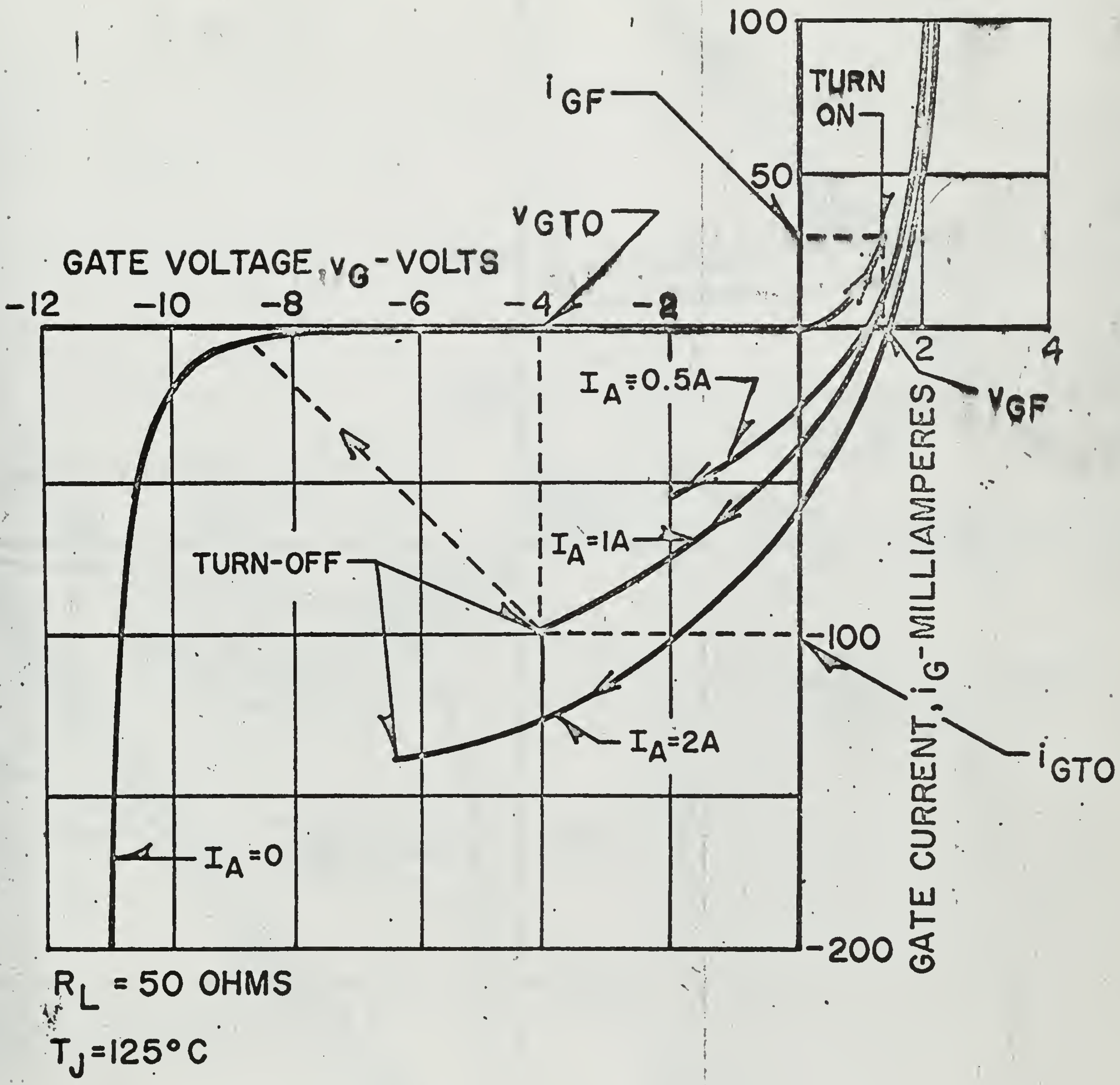

Typical Gate Characteristics of the WX241W Turn-Off TRINISTOR Controlled Rectifier

Fig. I-4

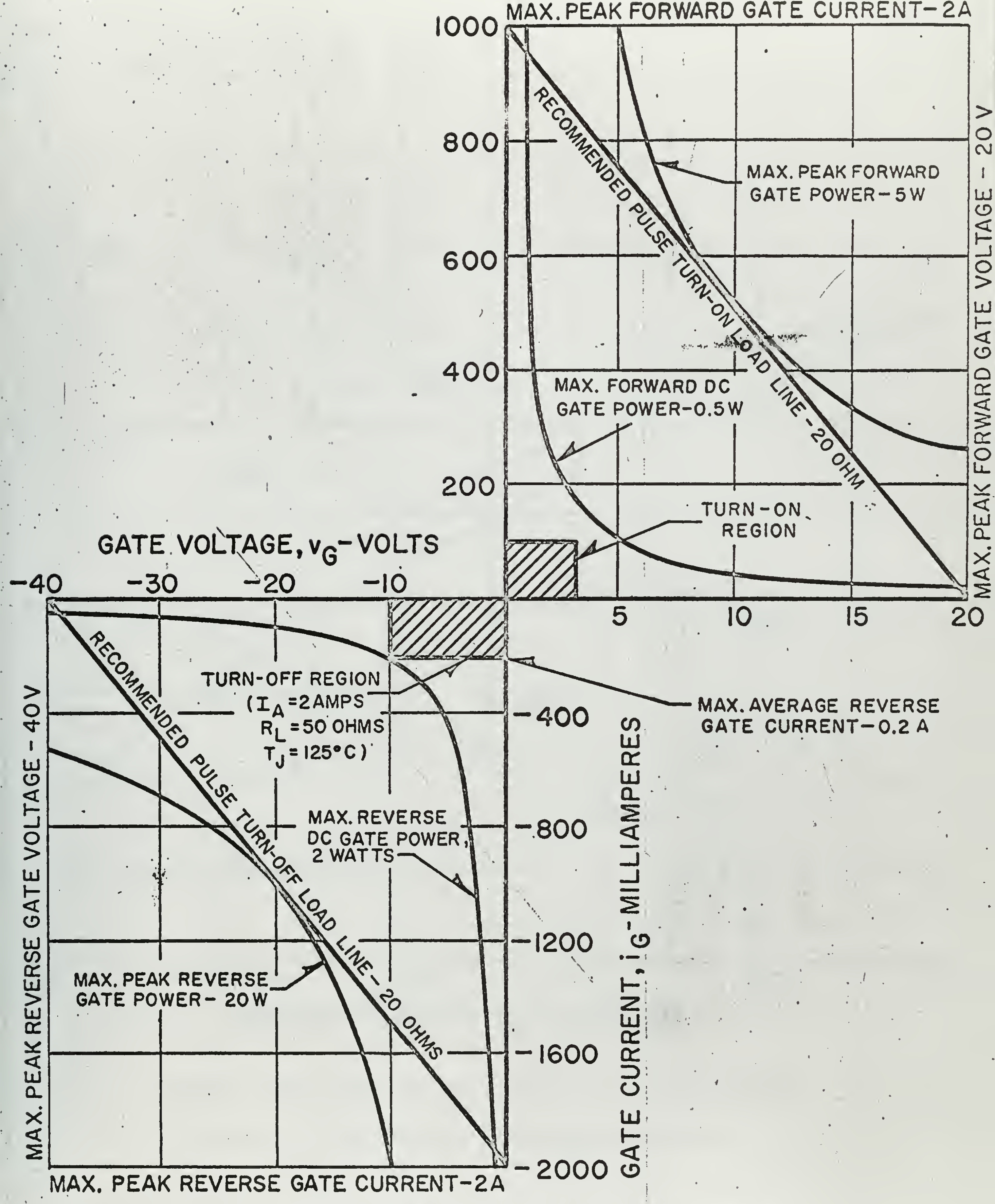

Gate Characteristics of the WX241W

Turn-Off TRINISTOR Controlled Rectifier

Fig. I-5

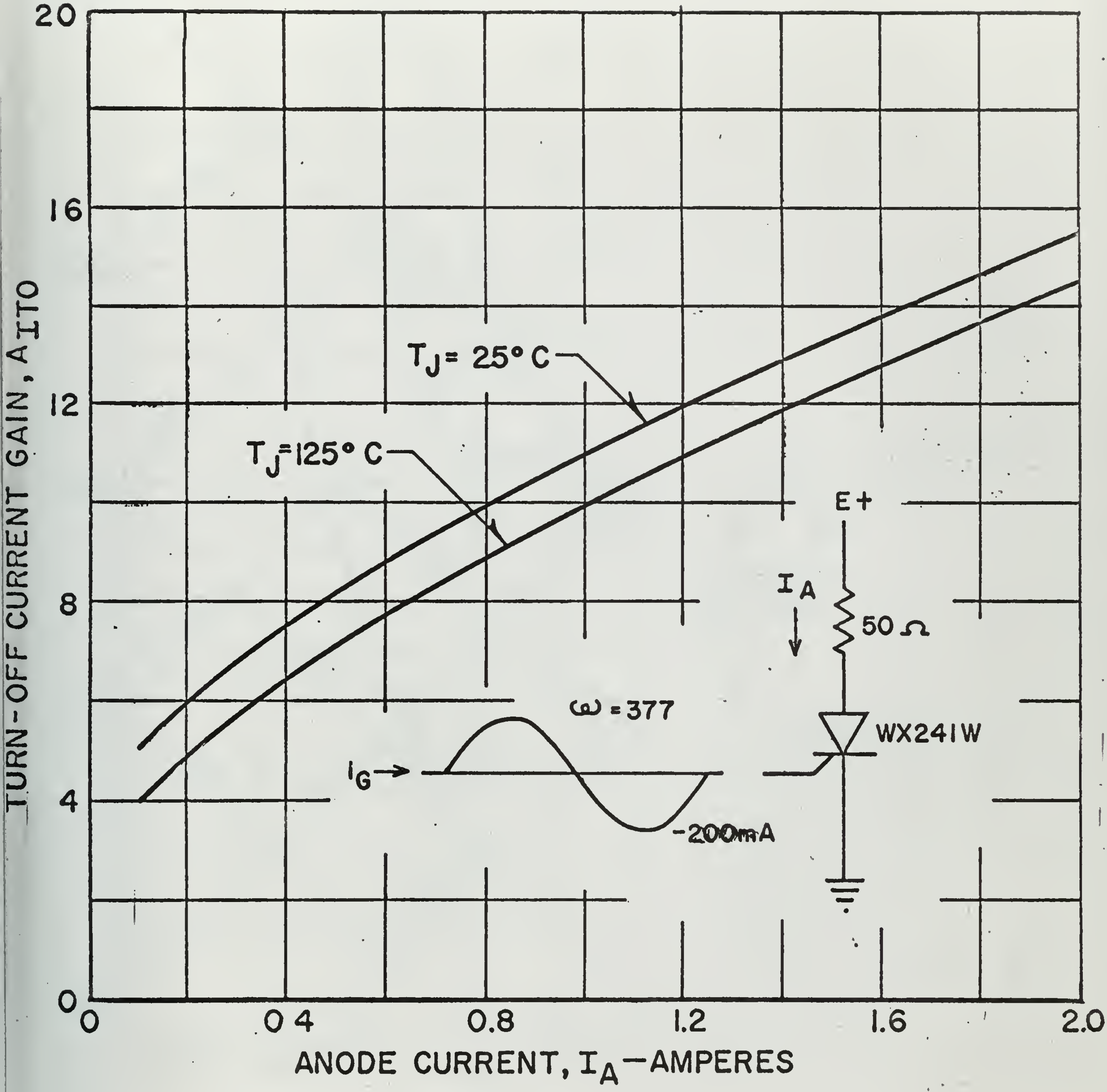

Typical Turn-Off Current Gain for the WX241W Turn-Off TRINISTOR Controlled Rectifier

Fig. I-6

[illegible]

[illegible]

[illegible]

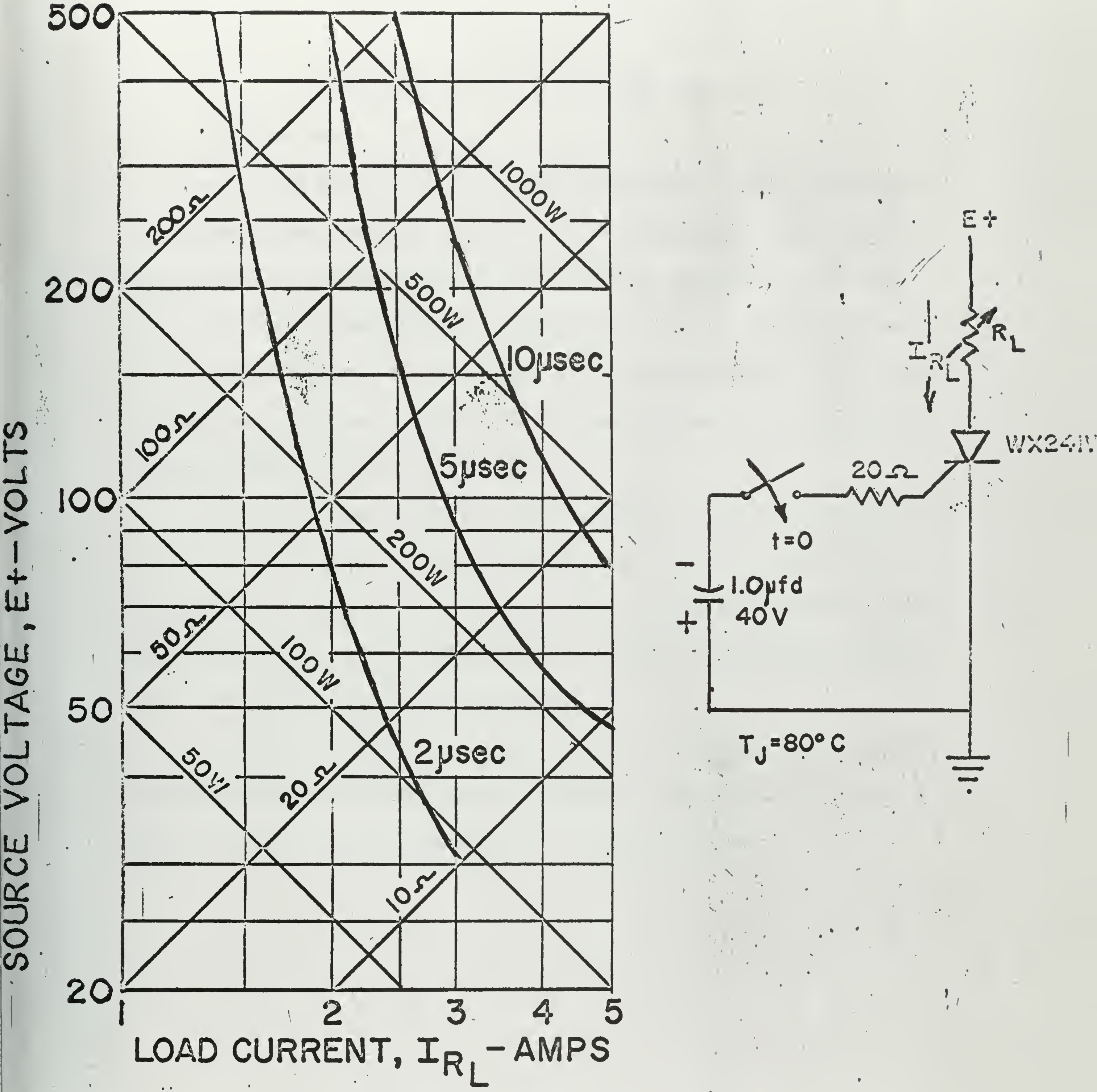

Typical Pulse Gate Drive Turn-Off Characteristics of the WX241W Turn-Off TRINISTOR Controlled Rectifier

Fig. I-7

CHAPTER TWO

AN ANALYSIS OF THE BASIC POWER AMPLIFIER

II.1 Introduction.

Due to its high switching efficiency, and fast switching ability it was felt that the gate turn-off controlled rectifier, GTCR, might be utilized in an amplifier circuit where the preservation of wave shape was unimportant, and the emphasis was on power amplification, efficiency and frequency correspondence. Accordingly, a basic inverter circuit employing two (2) GTCR's and a center tapped transformer as shown in Figure II-1 was investigated.

In part I of the Analysis, the amplifier was used with a simple resistive load and basic loop equations were written to solve for amplifier and load current, output voltage, power gain and efficiency. From these solutions an equivalent circuit was established to investigate loads considered in II-2 and III-1.

In each experimental circuit the in-put or triggering pulse was obtained from the circuit shown in Appendix I and was of 1.5 amps, peak amplitude, and approximately 10 μ sec duration.

II.2 Operation of the Ideal Circuit.

Consider the circuit shown below:

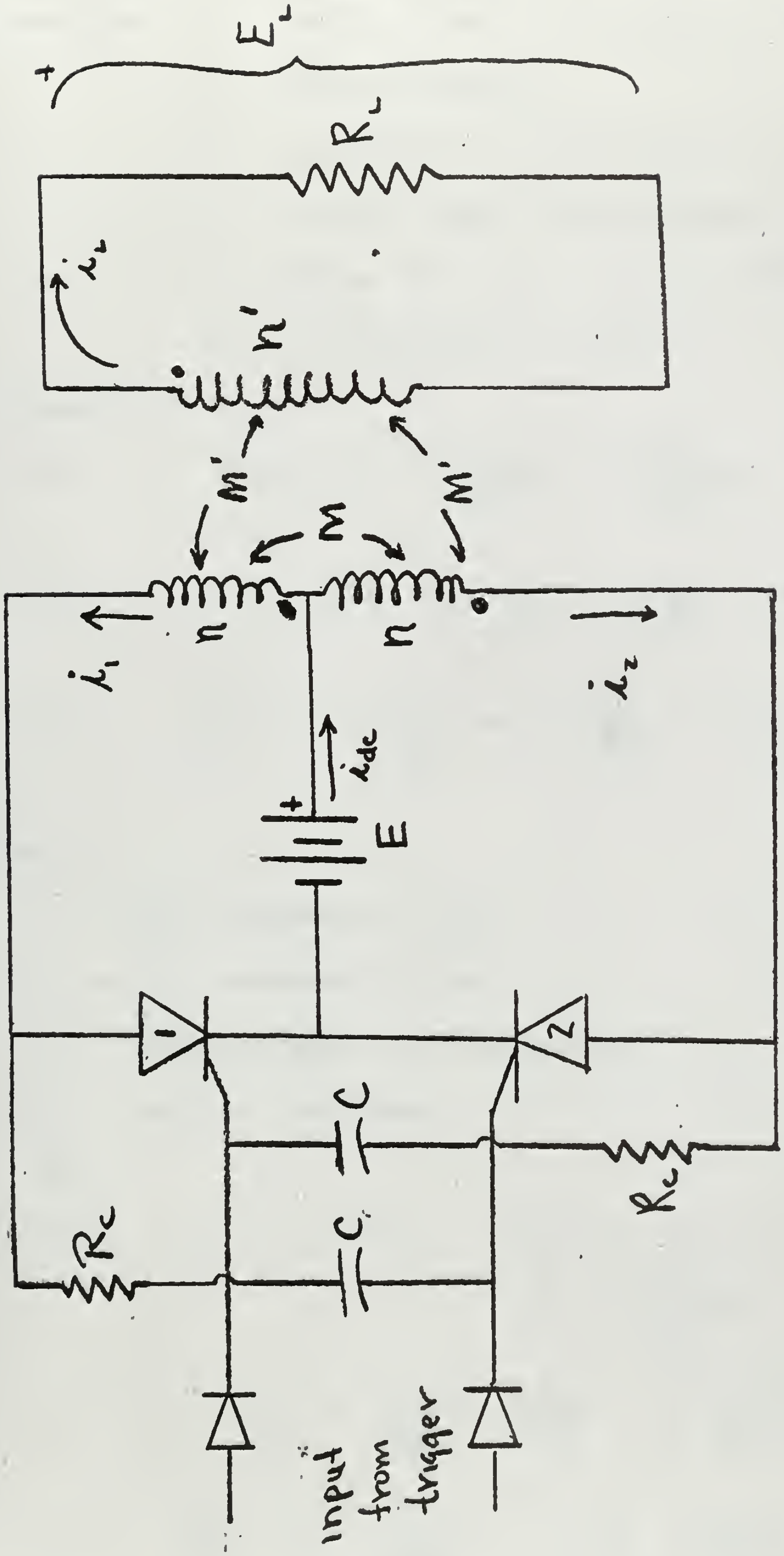

Fig. II-1 Operation of the Ideal Circuit

Assumptions:

1. Trigger pulse has no effect on load.
2. Matched components.
3. n = primary turns per loop n' = secondary turns

   $N = n/n'$, iron core transformer, $k \approx 1$
4. Voltage drop, V_o, across the conducting GTCR, $\approx$ 1 volt
5. # 1 conducting, # 2 open

Loop equations

(1) $$E = V_o + L_1 \frac{di_1}{dt} - M \frac{di_2}{dt} - M' \frac{di_L}{dt}$$

(2) $$E = i_2 R_c + L_2 \frac{di_2}{dt} - M \frac{di_1}{dt} + M' \frac{di_L}{dt} + \frac{1}{C} \int i_2 \, dt$$

(3) $$0 = -M' \frac{di_1}{dt} + M' \frac{di_2}{dt} + L_L \frac{di_L}{dt} + i_L R_L$$

where:

L_1 = self inductance of loop 1

L_2 = self inductance of loop 2

L_L = self inductance of secondary loop

R_1 = the load resistance

(4)

with $k \approx 1$, and $M \approx L_1 \approx L_2$

$$M' = \sqrt{L_1 L_L} \approx \sqrt{M L_L}$$

$$L_L = \frac{n'\phi}{i_L} \approx \frac{n'}{\frac{n i_1}{n'}} \times \frac{n\phi}{n} = \frac{n'^2}{n^2} \times \frac{n\phi}{i_1}$$

but $\dfrac{n'^2}{n^2} = \dfrac{1}{N^2}$ and $\dfrac{n\phi}{i_1} = L_1 \approx M$

therefore $L_L \approx \dfrac{L_1}{N^2} \approx \dfrac{M}{N^2} \approx \dfrac{L_2}{N^2}$ and $M' \approx \dfrac{M}{N}$

(5) adding (1) + (2) and using $L_1 \approx M \approx L_2$

$$2E - V_o = i_2 R_c + \frac{1}{c}\int i_2\,dt$$

expressing 5 in LaPlace transform: we get (6)

(6)

$$\frac{(2E - V_0)}{S} = I_2(S)R_c + \frac{1}{CS} I_2(S) + \cancelto{0}{\frac{1}{CS}\int^{0^+} i_2\,dt}$$

$$I_2(S) = \frac{(2E - V_0)}{R_c \left(S + \frac{1}{R_cC}\right)}$$

(7)

$$i_2(t) = \frac{(2E - V_0)}{R_c} \epsilon^{-\frac{t}{R_cC}}$$

now multiply (3) by N and add to 1

(1)

$$E = V_0 + L_1 \frac{di_1}{dt} - M\frac{di_2}{dt} - M'\frac{di_L}{dt}$$

$$N \times (3) = 0 = -M'N\frac{di_1}{dt} + M'N\frac{di_2}{dt} + NL_L\frac{di_L}{dt} + Ni_LR_L$$

but, $M'N \approx L_1 \approx L_2$ and $NL_L \approx M'$

(8) hence (1) + NX (3)

$$E - V_0 = Ni_LR_L \quad \text{or} \quad i_L = \frac{E - V_0}{NR_L}$$

(9) or assuming $i_{\text{magnetizing}} = 0$, $i_L \approx N(i_1 - i_2)$

and

$$i_1 = \frac{(E - V_0)}{N^2R_L} + \frac{(2E - V_0)}{R_c} \epsilon^{-\frac{t}{R_cC}}$$

$$i_{dc} = i_1 + i_2 = \frac{(E - V_0)}{N^2 R_L} + \frac{(4E - 2V_0)}{R_c} \epsilon^{-\frac{t}{R_c C}}$$

$$E_L = i_L R_L = \frac{E - V_0}{N}$$

(10) from (7) it is apparent that the maximum voltage across either GTCR is $2E-V_o$.

(11) the power in-put to the circuit is Power in $= I_{dc} E$

where $I_{dc} = i_{dc}$ average

$$i_{dc} = \frac{E - V_0}{N^2 R_L} + \frac{(4E - 2V_0)}{R_c T} \int_0^T \epsilon^{-\frac{t}{R_c C}} dt$$

(12) for

$$T \gg R_c C$$

$$I_{dc} = \frac{E - V_0}{N^2 R_L} + \frac{(4E - 2V_0)C}{T}$$

(13) Power output

$$P_o = I_L^2 R_L = \frac{E_L^2}{R_L} = \frac{(E - V_0)^2}{N^2 R_L}$$

(14) efficiency

$$\eta = \frac{P_{out}}{P_{in}} = \frac{\frac{(E - V_0)^2}{N^2 R_L}}{\frac{E - V_0}{N^2 R_L} + \frac{(4E - 2V_0)C}{T}}$$

(15) Power gain = $\dfrac{\text{Power Out-put}}{\text{Power required from trigger}}$

(16) For

$$\frac{E - V_0}{N^2 R_L} \gg \frac{(4E - 2V_0)C}{T}$$

$$I_{dc} \approx \frac{E - V_0}{N^2 R_L}$$

and maximum

$$\eta = 1 - \frac{V_0}{E}$$

if $E = 30$ volts and $V_0 = 1$ volt, $\eta_{max} = 0.967$

Taking the current equations

$$i_1 = \frac{E - V_o}{N^2 R_L} + \frac{(2E - V_o)}{R_c} \epsilon^{-\frac{t}{R_c C}}$$

and

$$i_2 = \frac{(2E - V_o)}{R_c} \epsilon^{-\frac{t}{R_c C}}$$

$$i_{dc} = i_1 + i_2 = \frac{E - V_o}{N^2 R_L} + \frac{(4E - 2V_o)}{R_c} \epsilon^{-\frac{t}{R_c C}}$$

Since $E \gg V_o$ neglect V_o

then

$$i_{dc} = \frac{E}{N^2 R_L} + \frac{E}{\frac{R_c}{4}} \epsilon^{-\frac{t}{R_c C}}$$

The equivalent circuit for these equations is shown below:

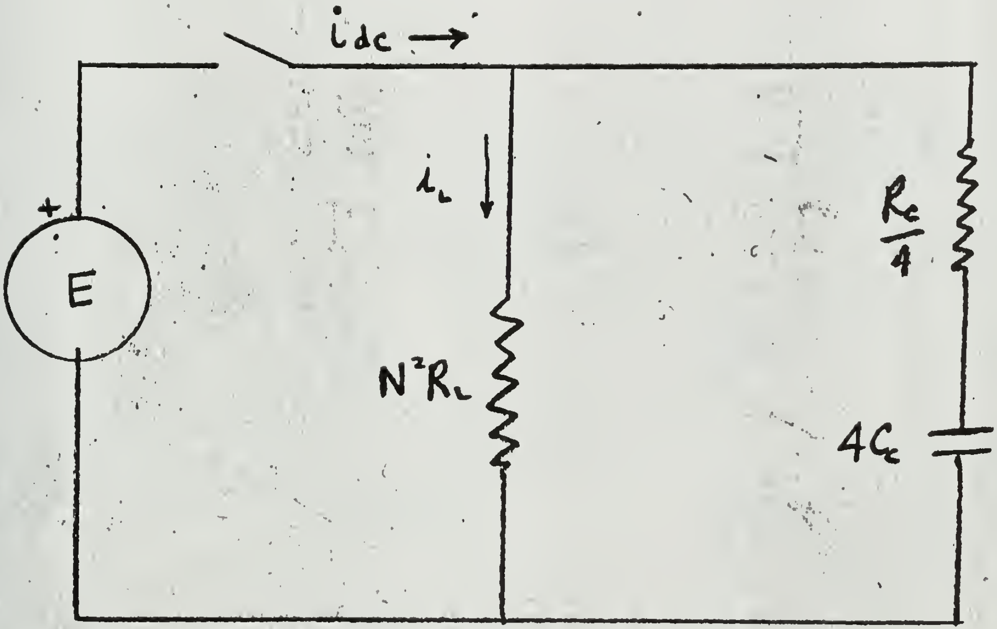

Fig. II-2

II-3 Analysis of the Experimental Circuit.

If we examine Figure II-4, which is the experimental setup for the basic amplifier circuit, we note that to correctly obtain a good comparison between calculated and observed results we must include in the calculated results the effect of the balancing resistors R_1 and R_2 and the inductance, I_L, associated with the load resistor R_1. We can introduce these parameters into our equivalent circuit as shown in Figure II-3.

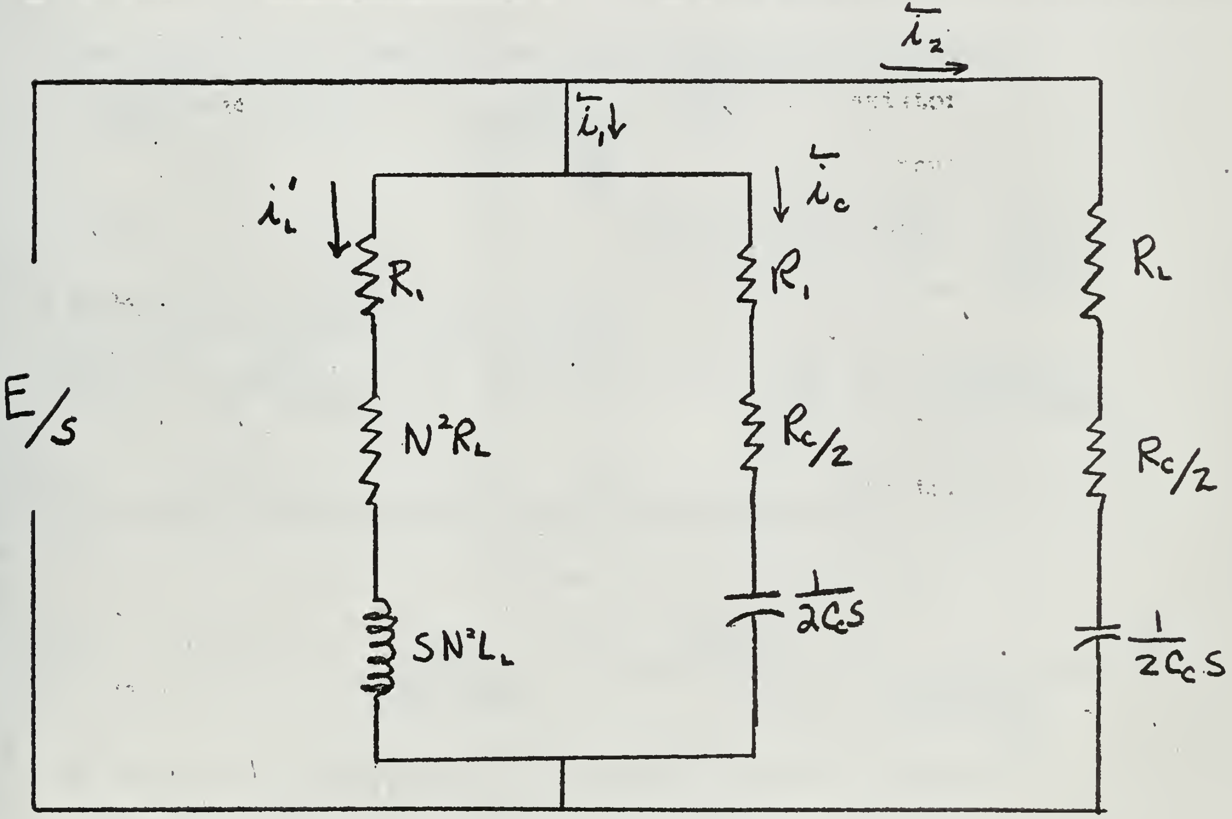

Fig. II-3.

We can use the LaPlace Transform directly, for step inputs: $E(s) = \frac{E}{S}$

and since $R_1 \approx R_2$

$$I_c(s) = I_2(s) = \frac{E}{S} \quad \frac{1}{R_1 + \frac{R_c}{2} + \frac{1}{2C_c S}}$$

$$I_c(s) = I_2(s) = \frac{E}{R_1 + \frac{R_c}{2}} \quad \frac{1}{s + \frac{1}{2C_c\left(R_1 + \frac{R_c}{2}\right)}}$$

and the load component reflected into the primary will be,

$$I_L'(s) = \frac{E}{N^2 L_L} \quad \frac{1}{s\left(s + \frac{R_1 + N^2 R_L}{N^2 L_L}\right)}$$

the time domain solutions for current can then be shown as:

$$i_c(t) = i_2(t) = \frac{E}{R_1 + \frac{R_c}{2}} \epsilon^{-\frac{t}{\tau_1}}$$

$$\tau_1 = 2C_c\left(R_1 + \frac{R_c}{2}\right)$$

and the load current in the primary

$$i_L'(t) = \frac{E}{R_1 + N^2 R_L}\left(1 - \epsilon^{-\frac{t}{\tau_2}}\right), \qquad \tau_2 = \frac{N^2 L_L}{R_1 + N^2 R_L}$$

The current thru the conducting GTCR is the sum of $i_L' + i_c$

or

$$(21) \quad i_1(t) = \frac{E}{R_1 + N^2 R_L}\left(1 - \epsilon^{-\frac{t}{\tau_2}}\right) + \frac{E}{R_1 + \frac{R_c}{2}} \epsilon^{-\frac{t}{\tau_1}}$$

We can get the load current by reference to the secondary

where

$$I_L(s) = I_L'(s)\, N$$

Since the output voltage $E_L(s) = I_L(s)\left(R_L + sL_L\right)$

$$E_L(s) = \frac{E}{N L_L} \quad \frac{R_L + sL_L}{s\left(s + \frac{R_1 + N^2 R_L}{N^2 L_L}\right)}$$

this can be simplified to

$$E_L(s) = \frac{E R_L N}{R_1 + N^2 R_L} \frac{1}{s} - \frac{E R_L N}{R_1 + N^2 R_L} \frac{1}{(s + \frac{R_1 + N^2 R_L}{N^2 L_L})} + \frac{E}{N} \frac{1}{(s + \frac{R_1 + N^2 R_L}{N^2 L_L})}$$

We can now write the time response as the inverse transform

$$E_L(t) = \frac{E R_L N}{R_1 + N^2 R_L} (1 - \epsilon^{-\left(\frac{R_1 + N^2 R_L}{N^2 L_L}\right)t}) + \frac{E}{N} \epsilon^{-\left(\frac{R_1 + N^2 R_L}{N^2 L_L}\right)t}$$

II-4 Experimental Results for the Basic Power Amplifier.

The laboratory setup for the circuit shown in Figure II-1 is shown below:

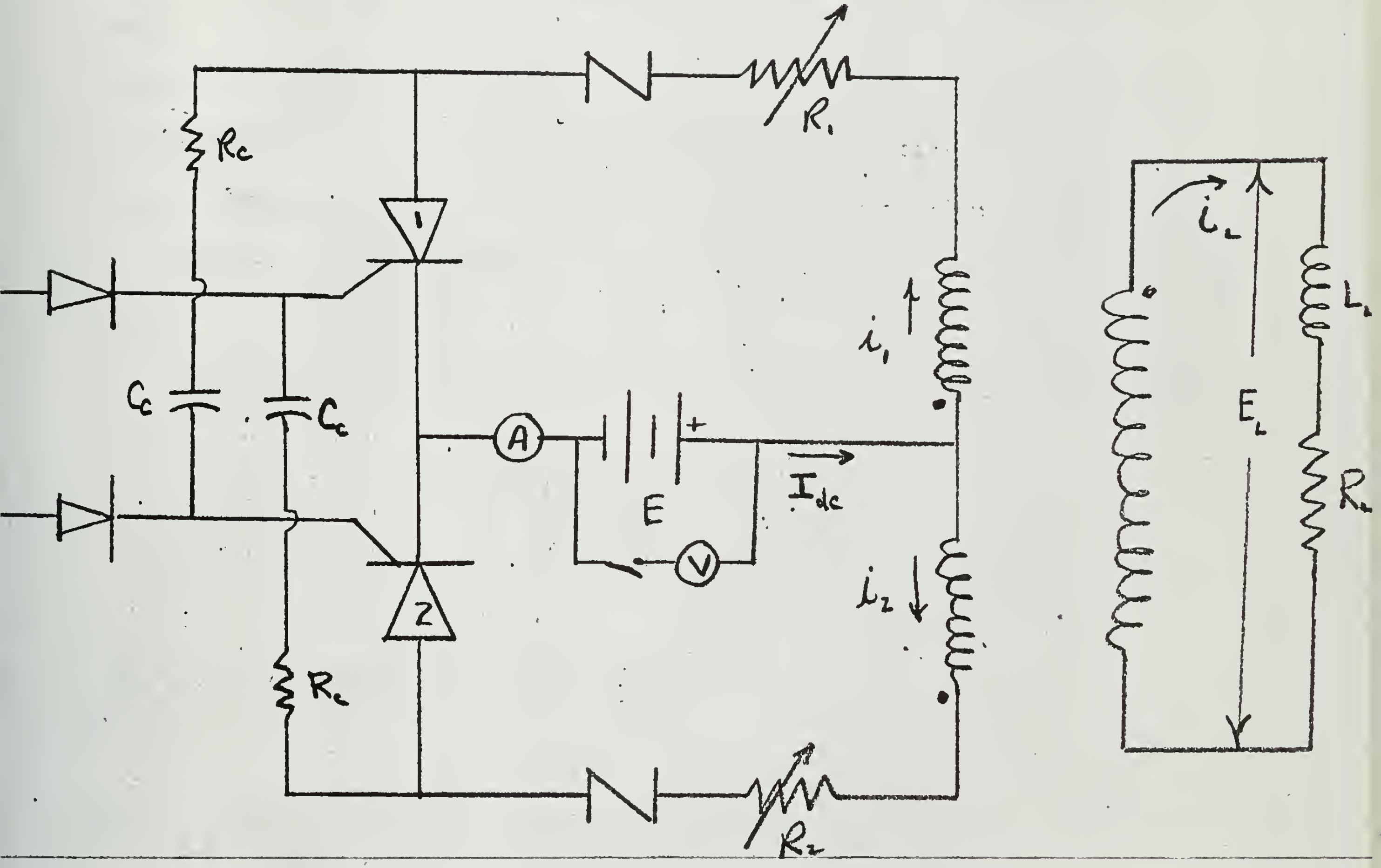

Fig. II-4

Parameters:

$E_L = 30$ volts
$V_o = 1$ volt
$N = \frac{1}{6}$
$N^2 = \frac{1}{36}$
$N^2 L_L = 2$ mh
$R_c = 30$ ohms
$C_c = .15\ \mu$ farads
$R_1 \simeq R_2 = 5$ ohms
$R_L = 1200$ ohms

It was found in the laboratory that without the resistors R_1 and R_2 shown in Figure II-4, the basic circuit would not operate. Analysis of the problem indicated that the transformer was saturating on the first half cycle, because a residual flux raised the level into the saturated region. Hence these resistors were needed to start the operation of the amplifier, and then to properly balance the output during each half cycle, which prevented a buildup of the flux level in either direction. If we could obtain perfectly matched components, at considerably more expense, it would be possible to shunt out these resistors completely after start up.

For the parameters given, the equations for predicted currents become:

$$i_2 = i_c = \frac{30}{5+15}\,\epsilon^{-\frac{t}{6\times 10^{-6}}}$$

$$= 1.5\,\epsilon^{-\frac{10^6 t}{6}} \quad \text{amperes}$$

the primary component of load current

$$i_L' = \frac{30}{5+\frac{1200}{36}}\left(1-\epsilon^{-\frac{38.6t}{2\times 10^{-3}}}\right) = .783\left(1-\epsilon^{-\frac{10^6 t}{51.8}}\right) \text{ amps.}$$

the current through the conducting GTCR

$$i_1 = i_L' + i_c = .783\left(1-\epsilon^{-\frac{10^6 t}{51.8}}\right) + 1.50\,\epsilon^{-\frac{10^6 t}{6}} \quad \text{amps}$$

the current from the source,

$$i_{dc} = i_1 + i_2$$

$$i_{dc} = .783\left(1-\epsilon^{-\frac{10^6 t}{51.8}}\right) + 3.0\,\epsilon^{-\frac{10^6 t}{6}} \quad \text{amps}$$

the average value of source current

$$I_{dc} = i_{dc_{ave}} = .783 - \frac{.783}{T} \int_0^T \epsilon^{\frac{-10^6 t}{51.8}} dt + \frac{3.0}{T} \int_0^T \epsilon^{\frac{-10^6 t}{6}} dt$$

for $T \approx 0.0005$ seconds

$$I_{dc} = .783 - .078 + .035 = 0.74 \quad \text{amperes}$$

Our calculated output voltage, E_L, becomes

$$E_L = \frac{(30)(1200)(\frac{1}{6})}{5 + \frac{1200}{36}} \left(1 - \epsilon^{\frac{-10^6 t}{51.8}}\right) + 180\, \epsilon^{-\frac{10^6 t}{6}}$$

which reduces to

$$E_L = 155.5 \left(1 - \epsilon^{-\frac{10^6 t}{51.8}}\right) + 180\, \epsilon^{-\frac{10^6 t}{6}} \quad \text{volts}$$

Power input = $.74 \times 30 = 22.20$ watts

Average current

$$I_{L_{ave}} = N i_{L_{ave}} = \frac{1}{6}(.783 - .078) = .1175 \text{ amps}$$

Output Power

$$P_{out} = (.1175)^2\, 1200 = 16.57 \quad \text{watts}$$

efficiency, $\eta_{cal} = \frac{16.57}{22.2} = 0.746$

In an attempt to obtain a better comparison of the predicted versus experimental results, the equations for the current, i_1, and the output voltage, E_1 can be solved by an analog computer. The analog circuits used are shown in Figures II-5 and II-6. The graphic solutions as shown in Figures II-7 and II-8 may be visually compared with the pictures taken

TABLE I

Table 1 presents for comparison the observed and calculated results. The calculations were based on the parameters listed and the equations derived above.

variable	**calculated**	**observed**	
i_1 =	$.785(1-e^{-10^6 t/51.8})+1.5e^{-10^6 t/6}$	$.80(1-e^{-t/T_1})+1.52e^{-t/T_2}$	amps
i_2 =	$1.50e^{-10^6 t/6}$	$1.52e^{-t/T_2}$	amps
Idc =	.74	.75	amps
E_L =	$155.5(1-e^{-10^6 t/51.8})+180e^{-10^6 t/51.8}$	$153(1-e^{-t/T_1})+180e^{-t/T_1}$	volts
Power input	22.20	22.50	watts
Power output	16.57	17.5	watts
Efficiency	0.746	0.778	
Power Gain	828	875	

of the observed variables shown in Figures II-9 and II-10.

For ease in the analog solution the equation for the current can be expressed by:

$$I_1(s) = \frac{E}{(R_1 + N^2 R_L)} \frac{1}{s\left(\frac{N^2 L_L s}{R_1 + N^2 R_L} + 1\right)} + \frac{E}{s\left(R_1 + \frac{R_c}{2}\right)} - \frac{E}{R_1 + \frac{R_c}{2}} \frac{1}{s\left(2C_c\left(R_1 + \frac{R_c}{2}\right)s + 1\right)}$$

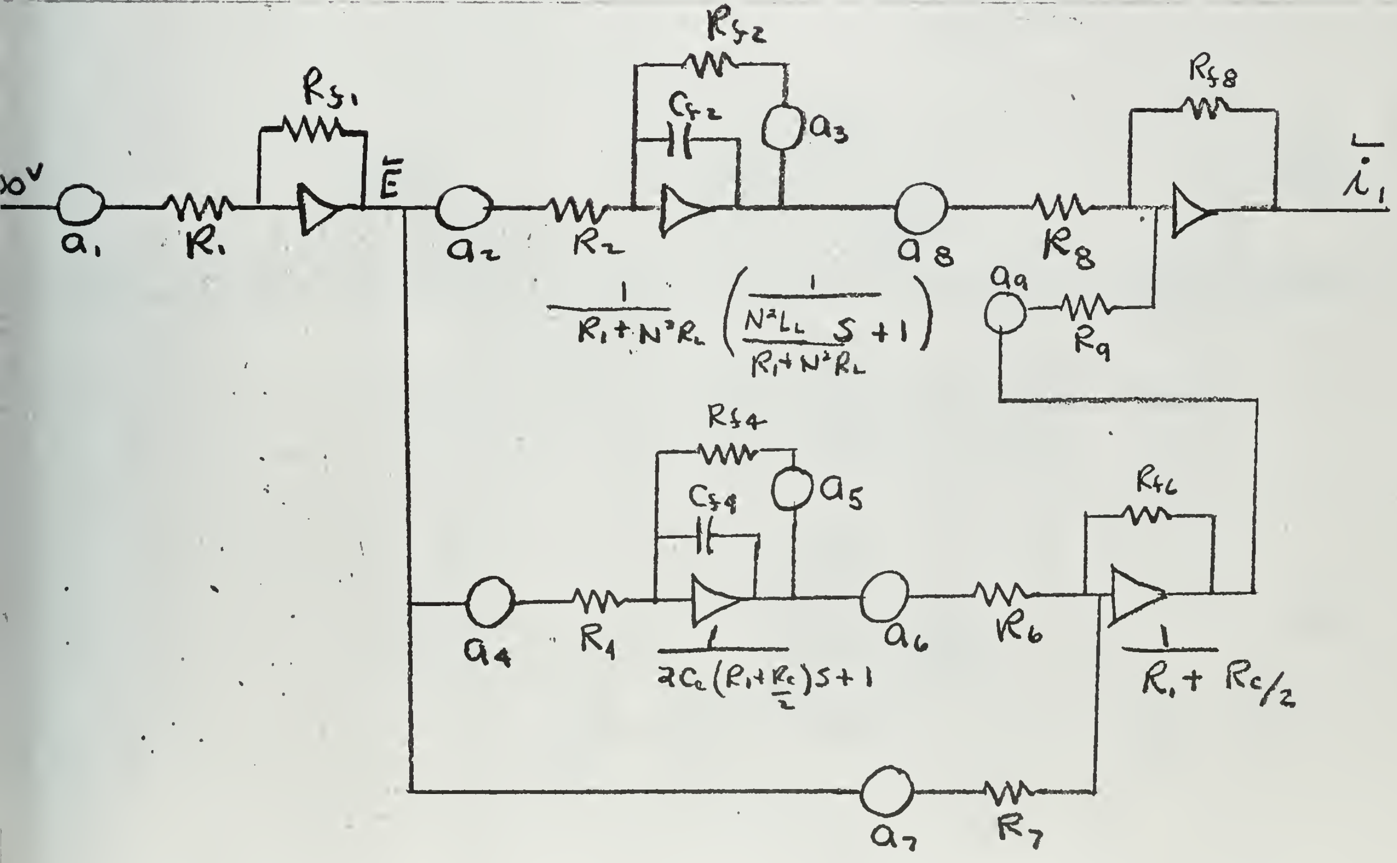

Fig. II-5

for parameters used:

and scaling factors $\alpha_E = 2$ $\alpha_i = .05$ $\alpha_t = 10^5$

$a_1 = .15$ $R_1 = R_{f1} = 1$ Meg-ohm

$a_2 = .199$ $a_3 = .192$ $R_2 = R_3 = 1$ Meg-ohm
$C_{f2} = 1$ microfarad

$a_4 = a_5 = .167$ $R_4 = R_5 = R_{f4} = 1$ Megohm
$C_{f4} = 1$ microfarad

$a_6 = a_7 = .5$ $R_6 = R_7 = .25$ Megohm, $R_{f6} = 1$ Megohm

$a_8 = a_9 = 1$ $R_8 = R_9 = R_{f8} = 1$ Meg ohm

similarly the output voltage equation can be expressed as:

$$E_L(s) = \frac{ENR_L}{(R_1 + N^2R_L)} \frac{1}{s\left(\frac{N^2L_L s}{R_1+N^2R_L} + 1\right)} + \frac{E}{NS} - \frac{E}{N} \frac{1}{s\left(\frac{N^2L_1 s}{R_1+N^2R_L} + 1\right)}$$

which can be solved as shown in Figure II-6.

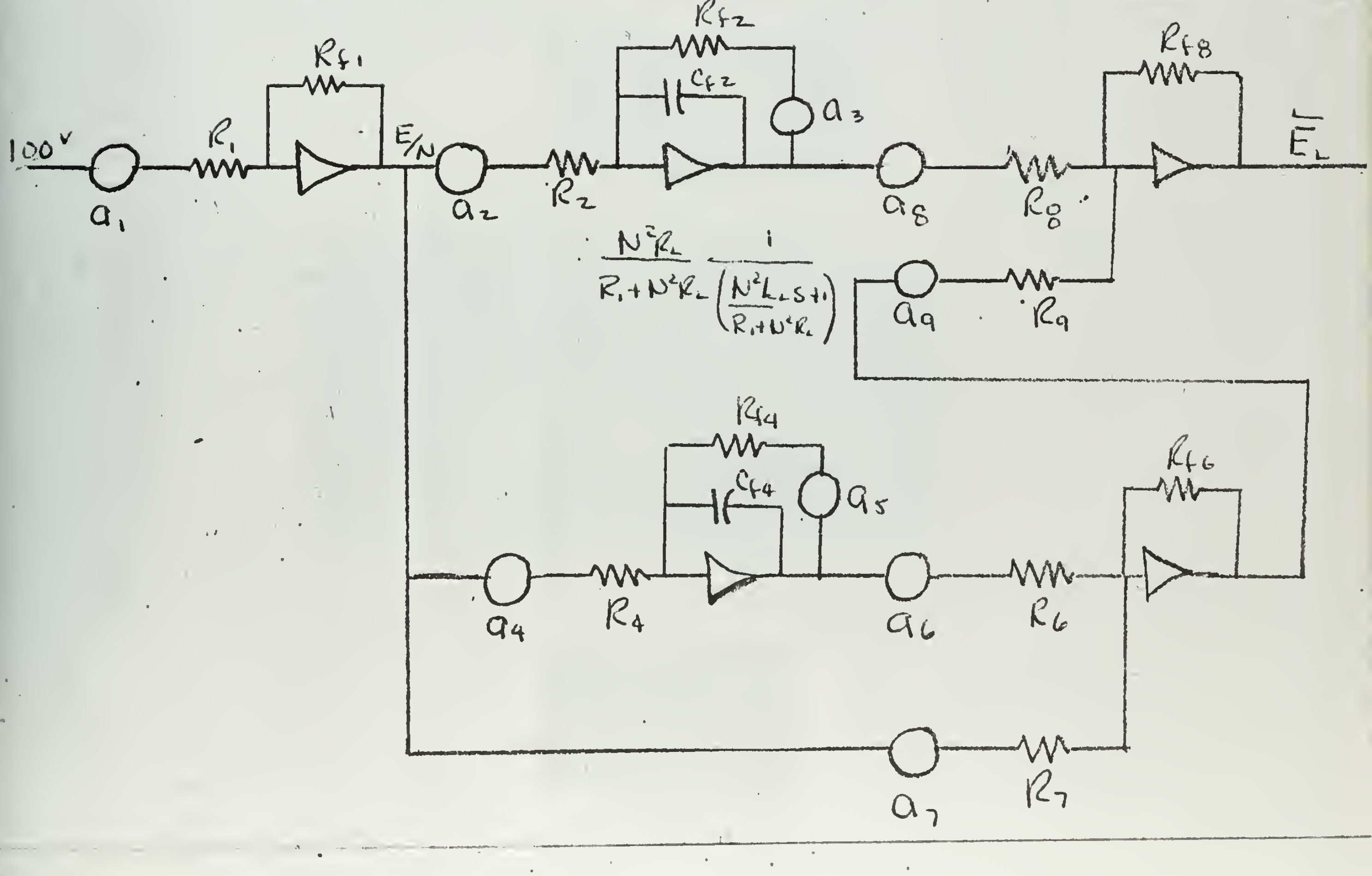

Fig. II-6

Analog Solution for Predicted Response of Amplifier

Scale:

vertical : 1 volt / line

horizontal : 1 mm/second

Scaling factors:

$\alpha_{time} = 10^5$ sec $\qquad \alpha_i = .05$ amps/volt $\qquad \alpha_v = 6$ volts/volt

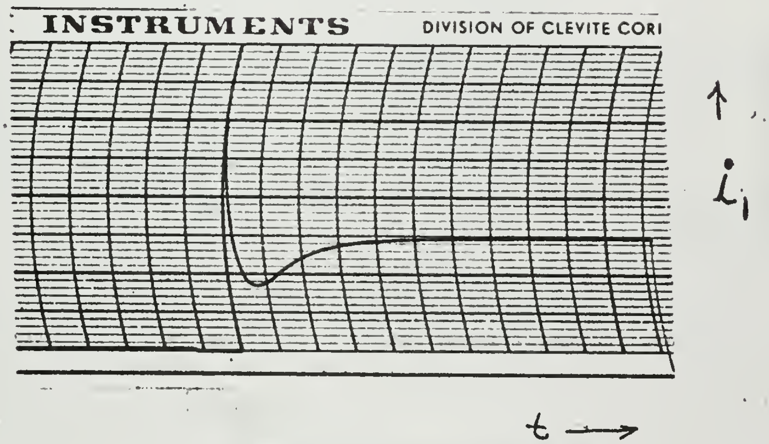

Fig. II-7

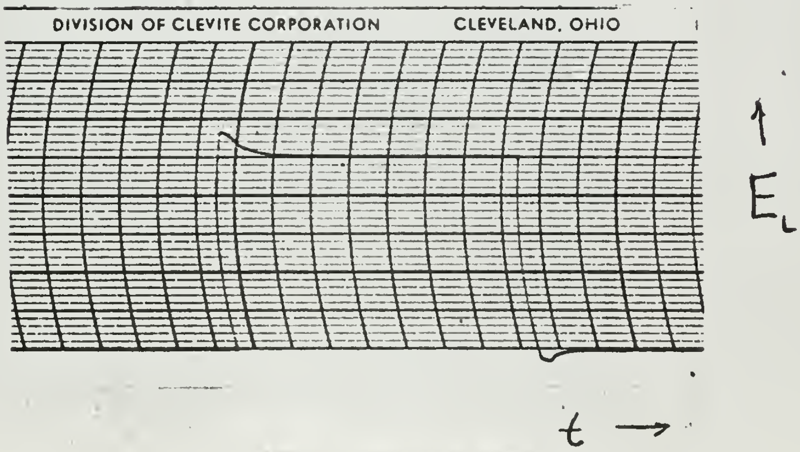

Fig. II-8

For the parameters given,

and letting $\alpha_E = 6$ $\alpha_t = 10^5$

$a_1 = .3$ $R_1 = R_{f1} = 1$ Meg-ohm

$a_2 = .5$ $R_2 = R_{f2} = 1$ Meg-ohm
$a_3 = .575$ $C_{f2} = 1$ microfarad

$a_4 = .575$ $R_4 = R_{f4} = 1$ Meg-ohm
$a_5 = .575$ $C_{f4} = 1$ microfarad

$a_6 = 1$ $R_6 = R_7 = R_{f6} = 1$ Meg-ohm
$a_7 = 1$

$a_8 = 1$ $R_8 = R_9 = R_{f8} = 1$ Meg-ohm
$a_9 = 1$

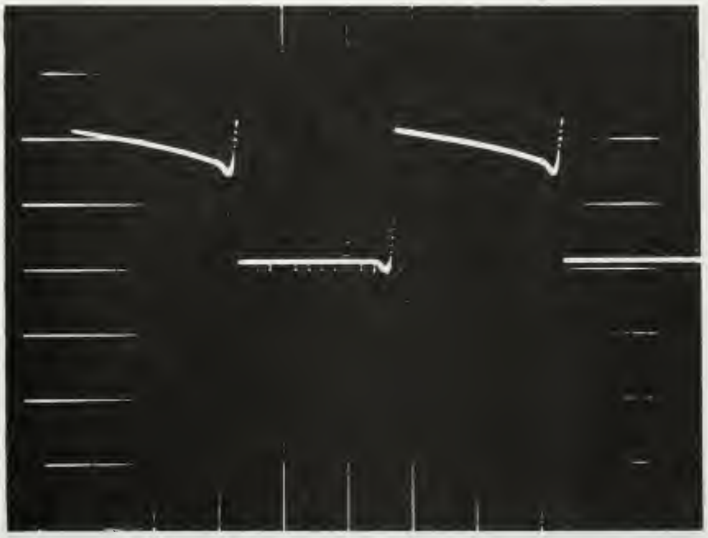

Fig. II-9

Amplifier Current vs Time

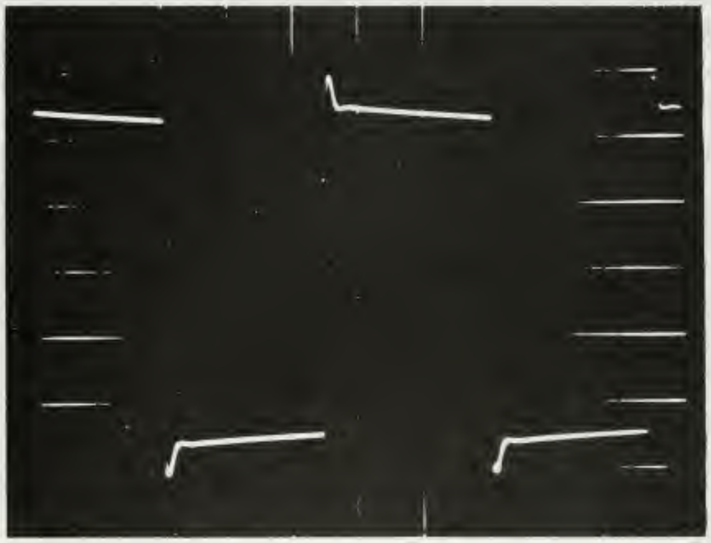

Fig. II-10

Output Voltage E_L vs Time

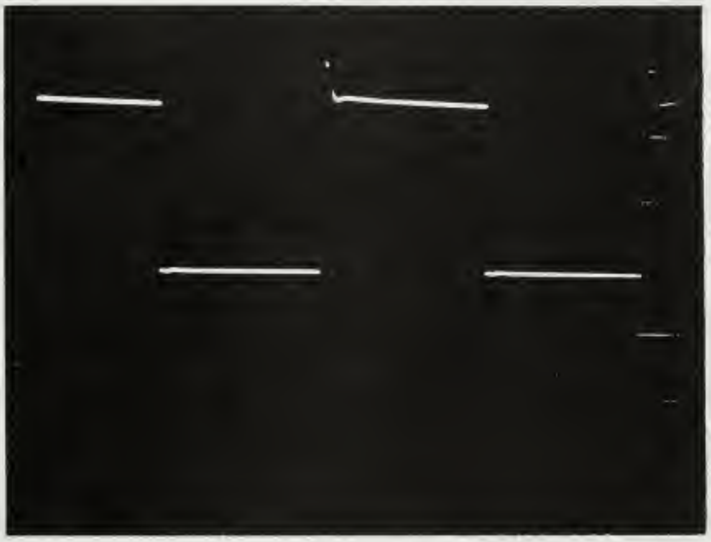

GTCR Voltage

1 cm = 20 volts

time

1 cm = 200 μsec

Fig. II-11

Voltage across GTCR vs Time

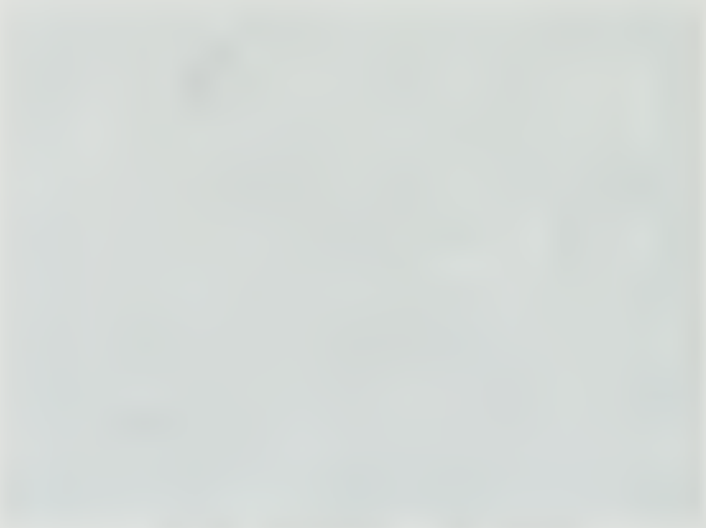

II-5 Discussion of Results.

In Section II-2 the basic assumptions which resulted in simplified solutions for i_1 and E_L were that the co-efficient of coupling k, was essentially unity and that the magnetizing current was negligible. The resulting equations then predicted the various wave shapes and values of the variables of interest, namely i_1, and E_L, in terms of the applied voltage E. Thus the voltage E could be selected to remain within the rated voltage of the GTCRs. The predicted maximum efficiency was 96.7% which is quite high, but if line and transformer losses are kept low it is felt that for a resistive load the efficiency will be greater than 90%. An important result of Section II-2 was the development of an equivalent circuit which greatly simplified the solutions for Sections II-3 and later work in Chapter Three where the load became more complex.

To examine the validity of the assumptions made in Part I, an experimental circuit was established as developed in Part II. This was the simplest form of the power amplifier which could be constructed with the material on hand. To more correctly compare the analytically predicted results with the observed results, another analysis was preformed which included the inductance inherent in the wire-wound power resistor used, and also the effects of the trimming resistances in each leg of the primary.

From the tabulated results we note that the calculated magnitudes agree very closely with the observed results, differing by less than 2% in each case. This deviation being well within the accuracy of the observed measurements which were obtained from an oscilloscope. In

conclusion then, it appears that the basic assumptions are valid and that the equivalent circuit is useful for varying loads. Since the solutions for amplifier current i_1, and output voltage E_L satisfy the observed amplitudes and wave shape they can be examined more closely to see what effect the varying of the parameter L_L will have on circuit operations. It can readily be shown that increasing L_L has little effect on E_L other than flattening the overshoot, however, when L_L is increased, the current i_1 will exhibit more undershoot, as indicated by equation (21). This is undesirable since if the undershoot drops below the rated holding current, and pulse gate drive is being used, the device will switch to the off position and the amplifier operations will be terminated. Thus for a fixed resistance there exists an upper limit of inductance which can be tolerated if the circuit is to function.

CHAPTER THREE

THE POWER AMPLIFIER WITH A TRANSDUCER LOAD

III.1 Introduction.

Now that we have developed an equivalent circuit and shown that it will predict results which agree with observed results let us examine analytically and experimentally, amplifier performance when the complex load becomes a transducer.

Figure III-1 shows the equivalent load seen by the amplifier, where R_L and C are the transducer equivalent and L_L is a tuning coil in series with the load.

In electrical terms a basic loading problem inherent with the transducer, is a coupling effect which causes the capacitance, C, in the equivalent circuit to vary. Thus the amplifier in meeting the operational requirements below, must do so for a range of possible capacitance, C.

1. While the output voltage wave shape may be distorted, the amplifier must maintain frequency correspondence with the input signal.
2. The amplitude of the output voltage should remain nearly constant through the range of C employed.
3. High power gains at efficiencies on the order of 60% or greater are demanded.

There are several general forms of equivalent circuits for transducers which depend primarily on transducer construction and the frequencies to be employed. For our study let us consider a circuit whose general form is shown in Figure III-1.

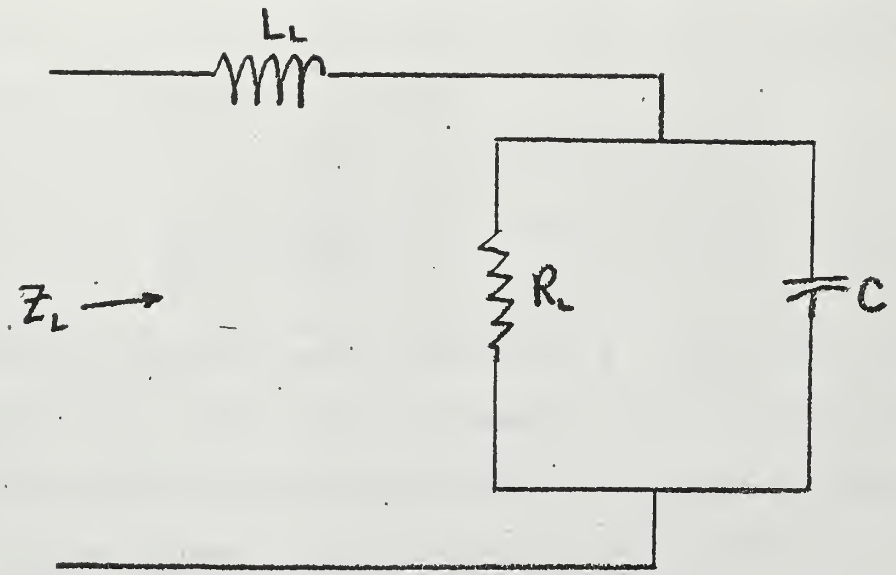

Fig. III-1

Since impedances are easily scaled in both magnitude and frequency so that laboratory models can be built to simulate existing circuits, the load simulated in the laboratory and used for our analytical results was based on values of R_L, L_L and C available. The objective then was to show the transient behavior when first L_L and R_L are kept constant while C varies, then keeping R_L and C constant the tuning coil was varied to note the damping effects, if any, introduced in the circuit.

It is important that we have some indices which reflect the relative bearing of the three parameters in order to investigate possible transient behavior. If we examine Figure III-1 we note that,

$$Z_L(s) = sL_L + \frac{R_L}{R_LCs+1}$$

which simplified is:

$$Z_L(s) = \frac{1}{R_LL_LC}\left(\frac{S^2 + \left(\frac{1}{R_LC}\right)S + \frac{1}{L_LC}}{R_LCS + 1}\right)$$

The numerator of this expression will occur in both the current and output voltage equations, and will in fact become the characteristic equation which will govern the response. Hence, this equation, of second order form, may in general be written:

$$S^2 + 2\xi\omega_n S + \omega_n^2$$

where $\xi = \frac{1}{2R_L}\sqrt{\frac{L_L}{C}}$ and $\omega_n = \sqrt{\frac{1}{L_L C}}$

Thus the parameters can be changed into ξ and ω_n ; indices for comparison with other possible parametric values. Additionally, since considerable analytical information has been gathered and evaluated on the transient response to step inputs for second order systems we can easily obtain information such as overshoot and rise time for given values of ξ and ω_n . Figures III-17 and III-18 for example can be used in the analytical calculations to predict rise times, t_p, and overshoot, M_{pt}.

III.2 Analysis of Transducer Loading.

In this analysis, let us first derive the equations for i_1, the current through the conducting GTCR, and the output voltage, E_L. The equation for E_L along with data on input power would then provide the necessary information regarding amplifier performance, and could also be reflected to the primary so that we can insure that $2E_L$ (primary) does not exceed the rated GTCR voltage. The resulting equation for i_1 would then tell us whether or not we exceed rated current and also indicate when the limits of pulse gate drive would be exceeded.

To obtain the desired solutions for i_1 and E_L we substitute the load circuit into the equivalent circuit developed in Chapter Two. The resulting circuit which we can attack analytically is shown in Figure III-2.

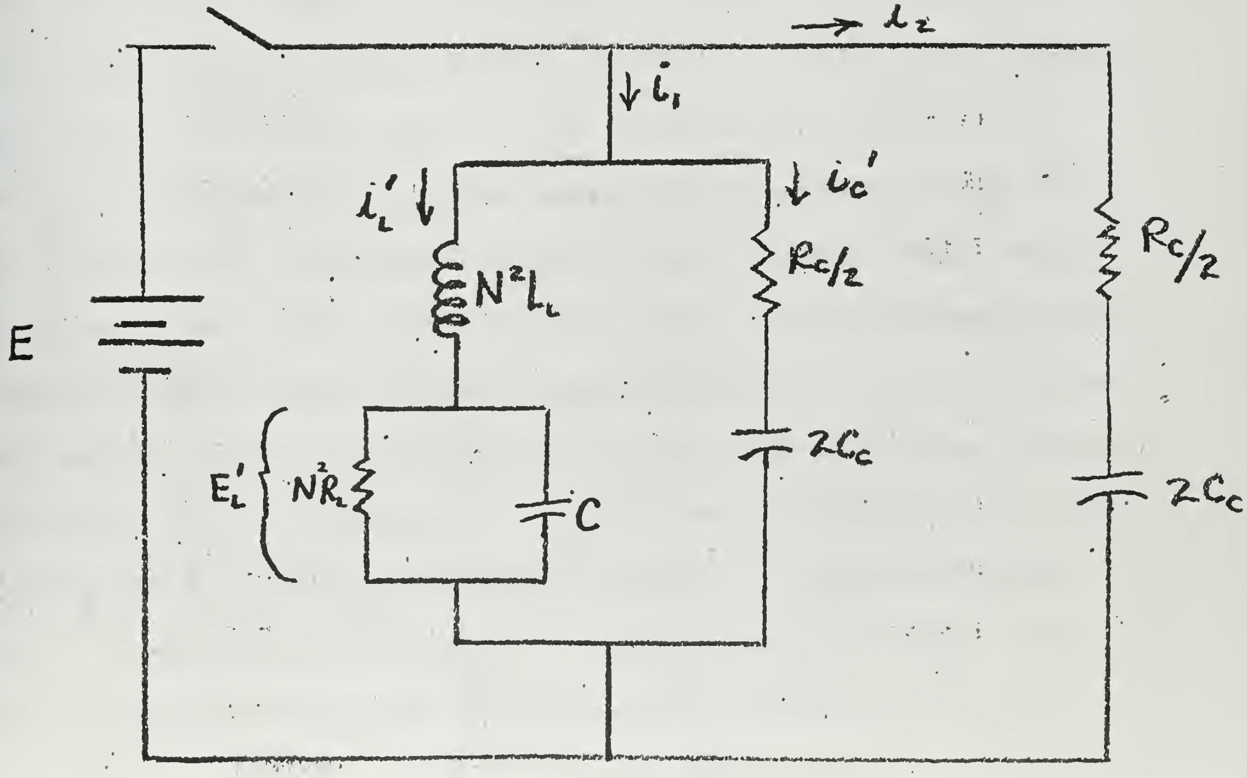

Fig. III-2

Solutions for i_1, the current through the conducting GTCR, and E_L the output voltage can be written directly in LaPlace Transforms.

$$I_1(s) = I_L'(s) + I_c'(s)$$

where $$I_L'(s) = \frac{E}{N^2} \quad \frac{(R_L C s + 1)}{s(R_L C L_L s^2 + L_L s + R_L)}$$

and $$I_c'(s) = \frac{E}{S} \quad \frac{2 C_c S}{R_c C_c S + 1}$$

$$\therefore \; I_1(s) = \frac{E}{N^2} \quad \frac{(R_L C s + 1)}{s(R_L C L_L s^2 + L_L s + R_L)} + 2 E C_c \quad \frac{1}{R_c C_c S + 1}$$

and $$E_L(S) = \frac{E R_L}{N} \quad \frac{1}{s(R_L C L_L S^2 + L_L S + R_L)}$$

The transient behavior of i_1 and E_L is of considerable importance in devising protective schemes for the circuit. A readily apparent problem is that of overshoots of both current and applied voltage which could destroy the GTCR's, or at least change their characteristics, if rated surge values are approached or exceeded. Another transient aspect that must be considered however, is the minimum value of current, i_1, attained during undershoot. Since pulse type triggering of about 10 μ-sec duration will probably be employed, so that maximum current can be controlled, the current through the device must never be allowed to drop below the rated holding current. Should this occur the device will be switched to the high resistance portion of its operating curve, and power to the load will be interrupted. Interruptions of this sort are harmful if they also bring about transformer saturation on the following half cycle. Transformer saturation is very harmful for this circuit since in the on condition the primary circuit contains virtually no impedance,

and large currents will flow in the primary until protective devices operate.

Now that expressions for both i_1 and E_L are available, perhaps the best and quickest means of observing the transients would be to simulate the current and output voltage transfer functions on the analog computer. We could then observe the response to a step input of E volts with R_L fixed and the parameters L_L and C being varied.

To simplify the analog solution for i_1, rearrange the equation so that:

$$I_1(s) = \frac{E}{R_L N^2} \frac{R_L}{s(R_L C L_L s^2 + L_L s + R_L)} + \frac{E R_L C s}{R_L N^2} \frac{R_L}{s(R_L C L_L s^2 + L_L s + R_L)} + \frac{E}{s} \frac{2C_c s}{(R_c C_c s + 1)}$$

let,

$$I_1(s) = I_1'(s) + I_1''(s) + I_c(s)$$

and

$$I_1'(s) = \frac{E}{N^2 R_L} \frac{R_L}{s(R_L C L_L s^2 + L_L s + R_L)}$$

$$I_1''(s) = \frac{E R_L C s}{N^2 R_L} \frac{R_L}{s(R_L C L_L s^2 + L_L s + R_L)} = R_L C s \, I_1'(s)$$

$$I_c(s) = \frac{E}{s} \frac{2 C_c s}{(R_c C_c s + 1)}$$

The analog circuit for the solution of i_1 is shown in Figure III-3. (See Appendix II for the details of scaling)

Next write the equation for output voltage:

$$E_L(s) = \frac{E}{N} \frac{R_L}{s(R_L C L_L s^2 + L_L s + R_L)}$$

which in transfer function form is

$$\frac{E_L(s)}{E/N} = \frac{R_L}{R_L C L_L s^2 + L_L s + R_L}$$

For analog simulation consider then that

$$\frac{R_L}{R_L C L_L s^2 + L_L s + R_L} = \frac{F_o}{1 + F_o}$$

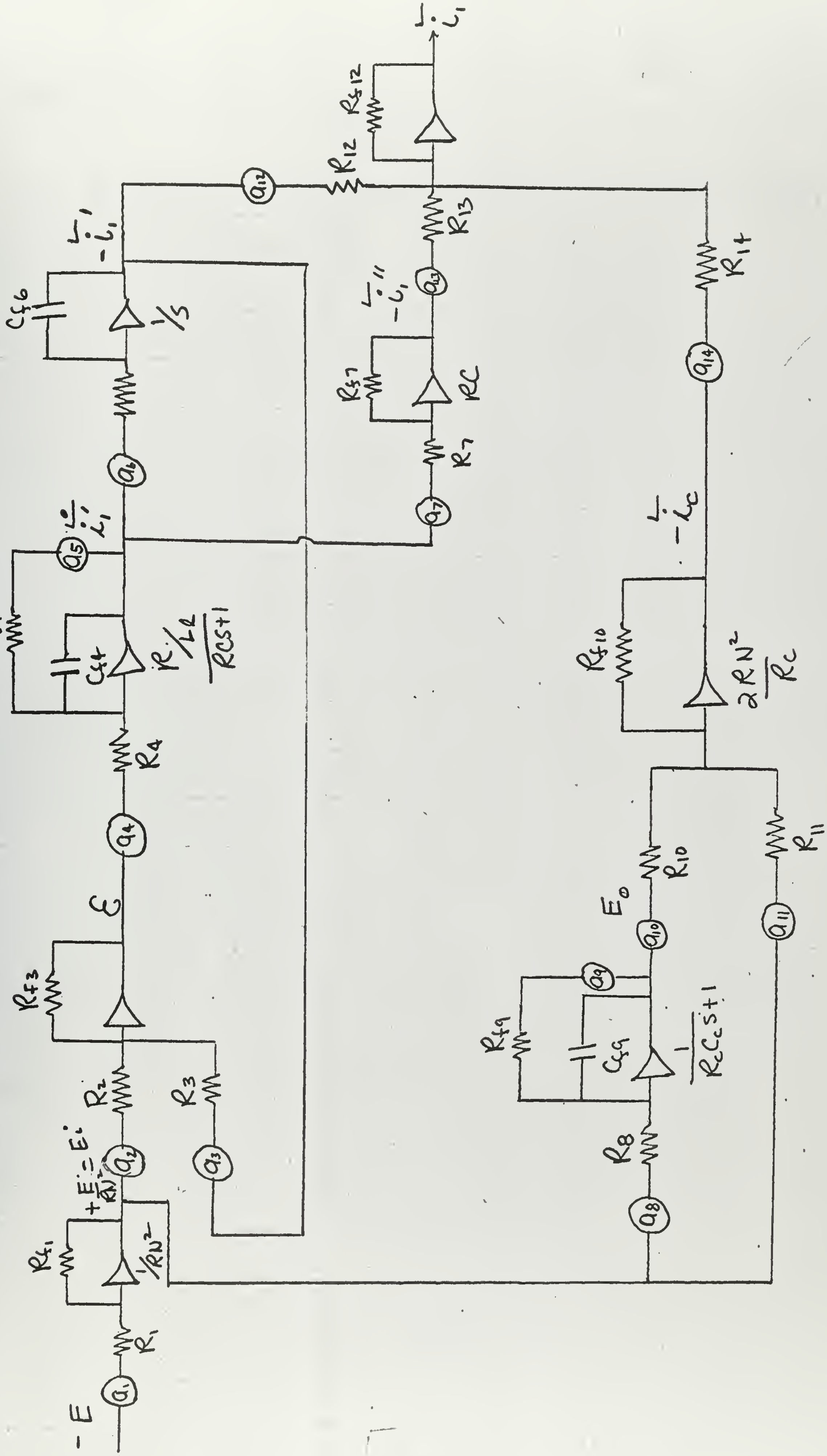
-E
a1
R1
Rf1
1/RN²
+E/RN² = E'
a2
R2
a3
R3
Rf3
ε
a4
R4
Rf4
Cf4
(R/L2)/(RCs+1)
a5
i1'
a6
Cf6
1/s
-i1'
a12
R12
Rf12
i1
R13
a13
-i1''
Rf7
RC
R7
a7
R14
a14
-ic
Rf10
2RN²/Rc
R10
R11
E0
a10
a11
a9
Rf9
Cf9
1/(RcCcs+1)
R8
a8

Fig. III-3

where $$F_o = \frac{R_L / L_L}{s(R_L C s + 1)}$$

which becomes the open loop transfer function in the feedback analog circuit shown in Figure III-4.

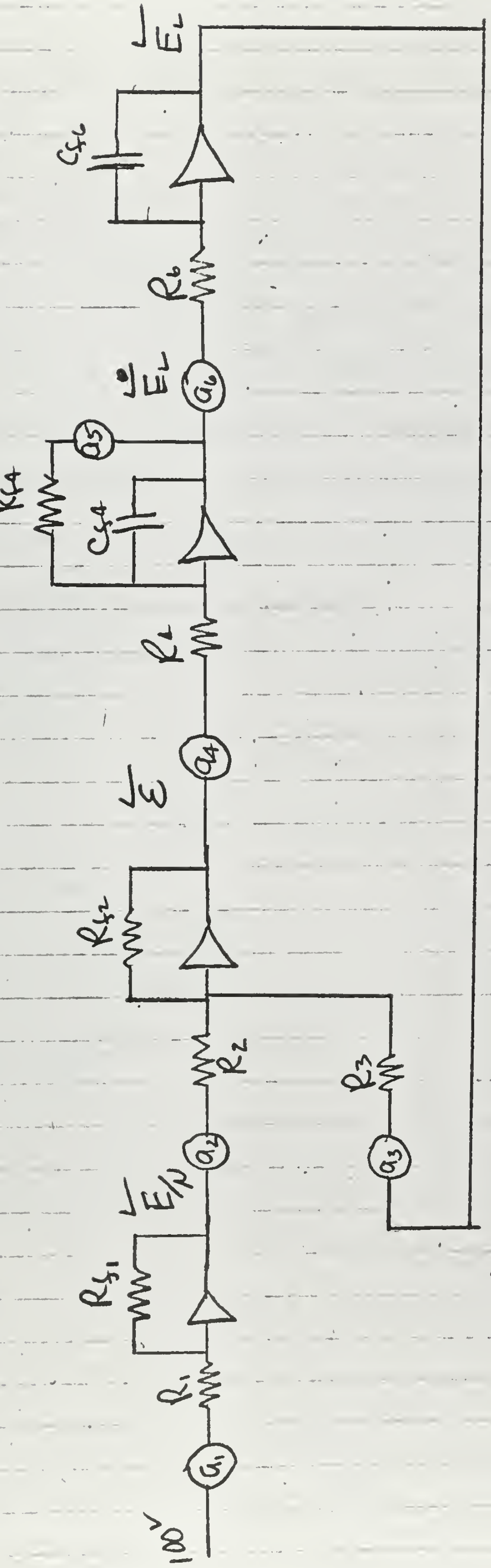

Fig. III-4

III.3 Discussion of Analytical Results.

Figures III-5 through III-11 show the analytical results for R_L and L_L fixed and C varying. We note that the range of parameters used covers the range of $\xi = .95$ to $\xi = .302$. Both current and voltage wave shapes followed the expected pattern, being damped heavily near $\xi = .95$ and growing oscillatory as C was increased. At ξ's near 0.3 we can see that the system has grown quite oscillatory, and that our voltage overshoot is now greater than 30%, and our current undershoot is very pronounced. Hence were our parameters to vary in this manner, we could safely predict that for this range the current i_1 remains above 50 milliamperes, the approximate holding current, and that the overshoot of output voltage will not exceed 36%.

The parameters below and scaling factors apply to Figures III-5 through III-11.

$$R_L = 1440 \text{ ohms}$$

$$L_L = .016 \text{ henries}$$

for current curves:

$$\alpha_t = 9 \times 10^4$$

$$\alpha_{i_1} = .025$$

for voltage curves

$$\alpha_t = 54 \times 10^4$$

$$\alpha_{E_L} = 6$$

$c = 0.0021\ \mu f \qquad \xi = 0.95$

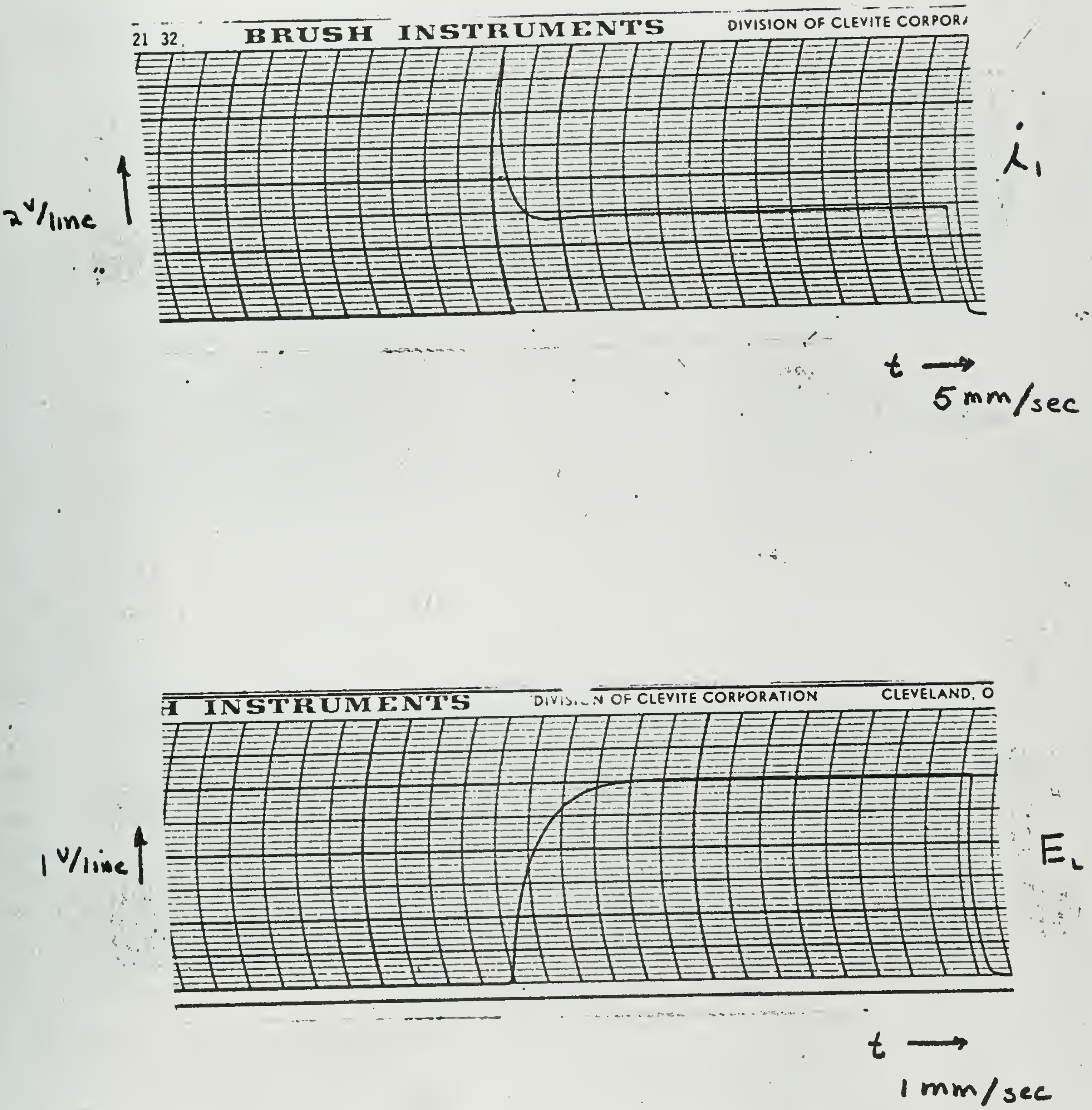

Fig. III-5

$C = 0.0042\ \mu f \quad \zeta = 0.678$

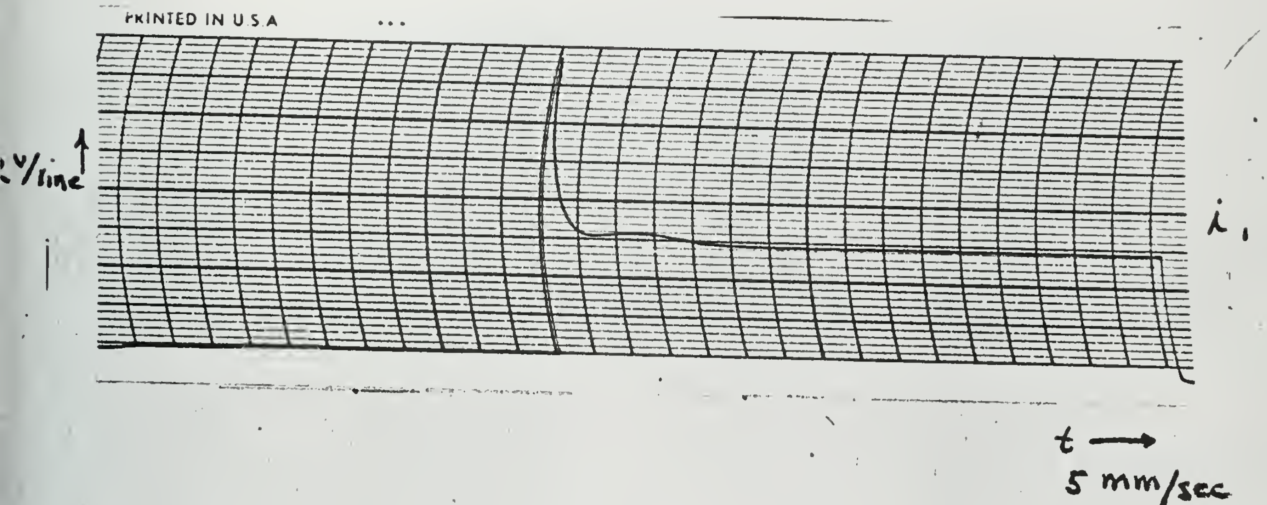

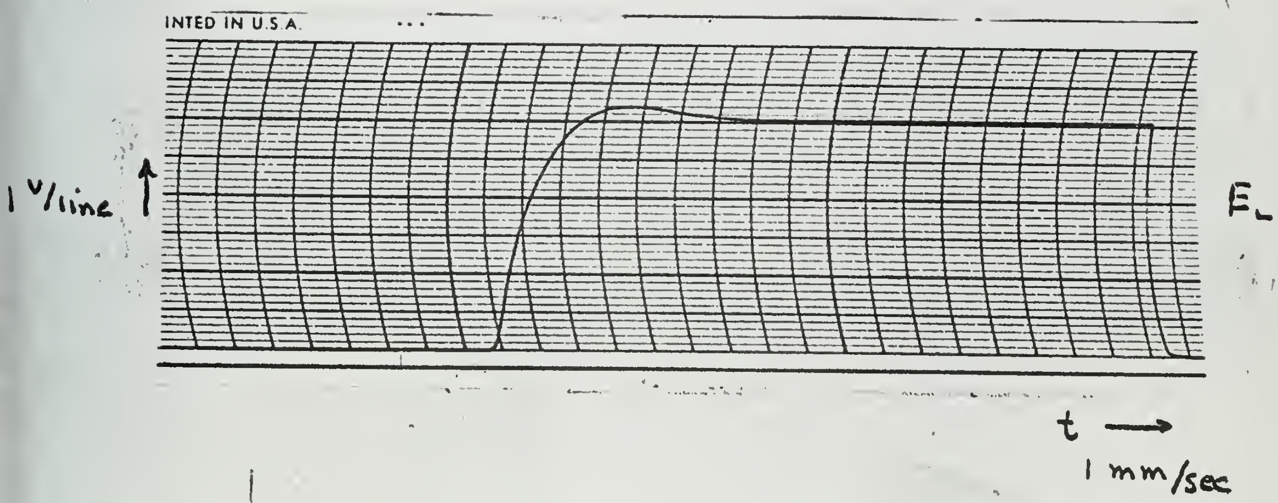

Fig. III-6

$C = 0.00612\ \mu f \qquad \zeta = 0.562$

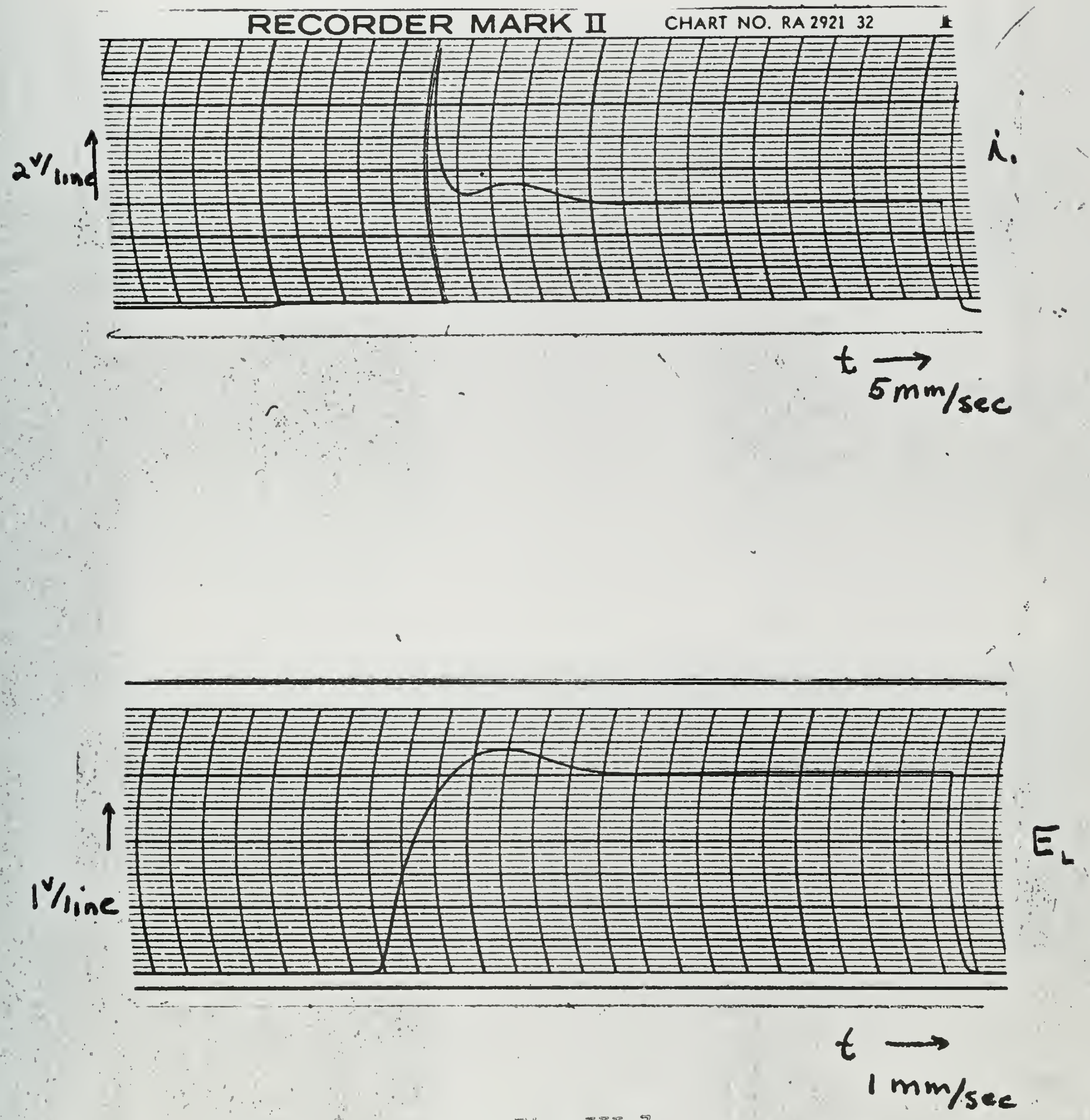

Fig. III-7

$C = 0.0082\ \mu f \quad \xi = 0.485$

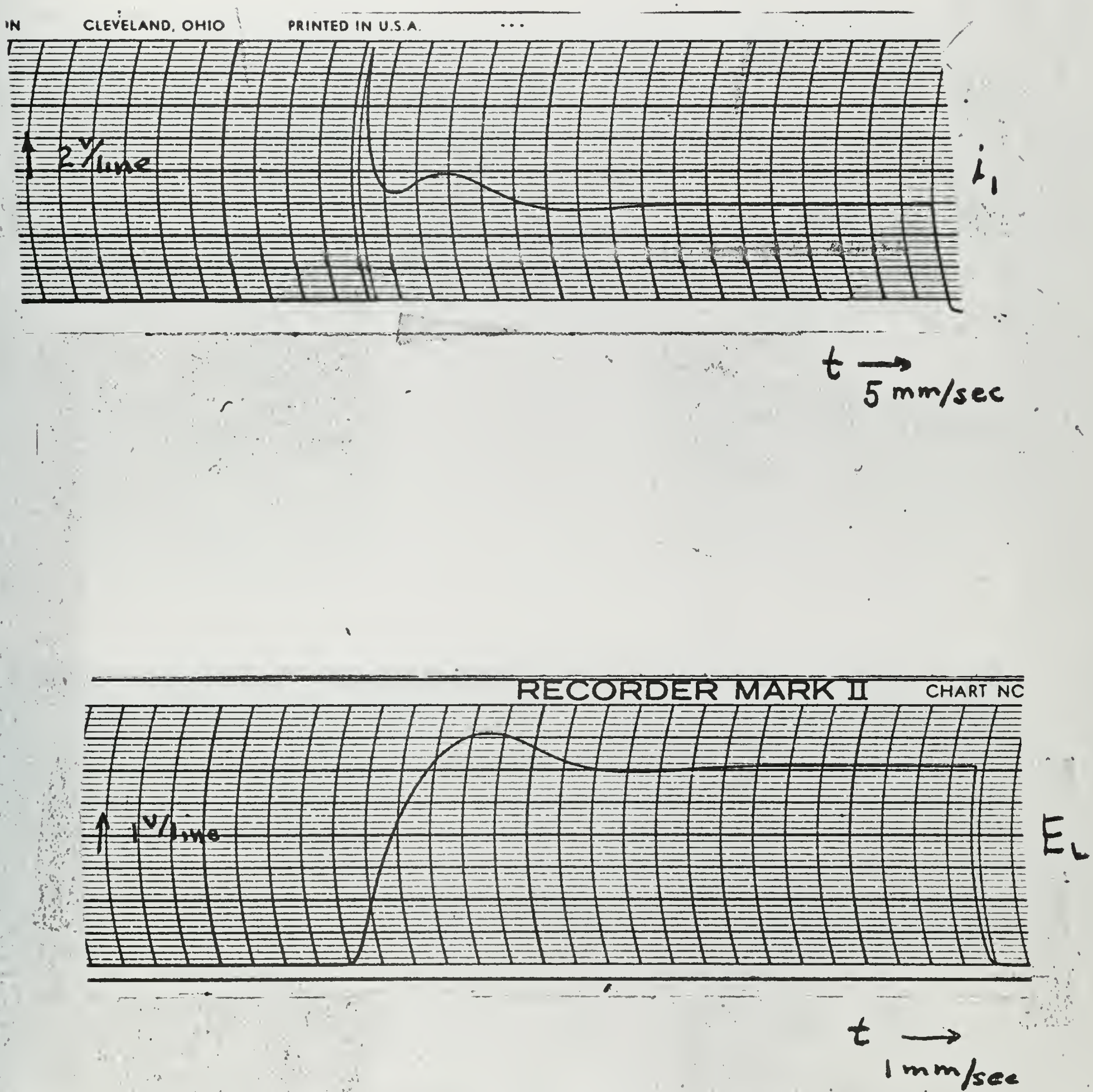

Fig. III-8

$C = 0.011\,\mu f$ $\xi = 0.418$

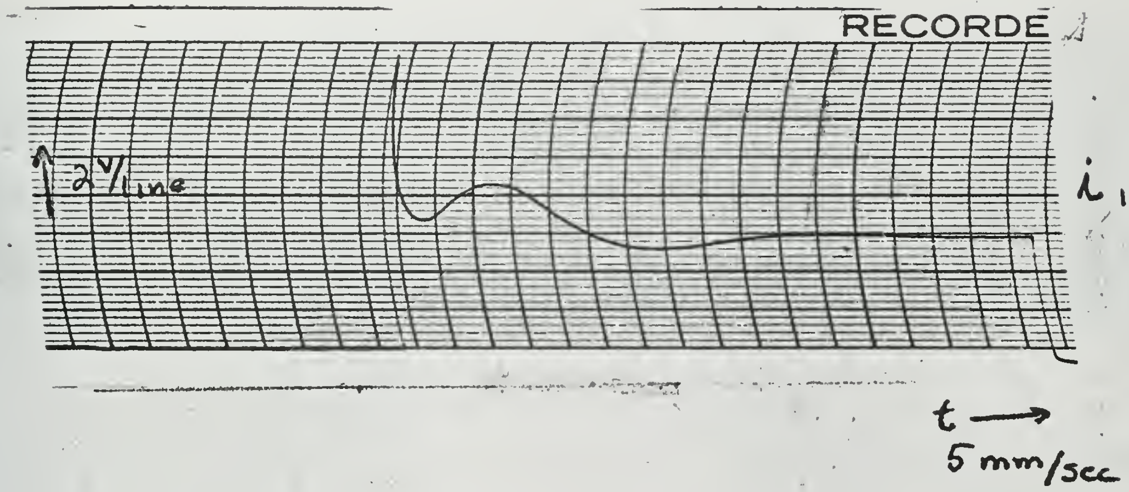

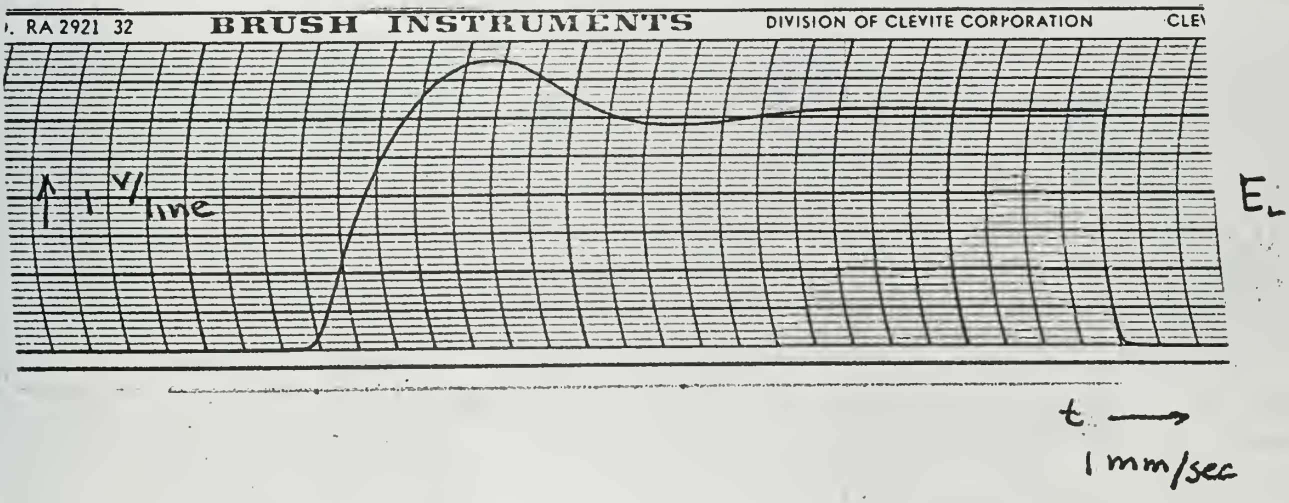

Fig. III-9

$C = 0.016\,\mu f \qquad \xi = 0.347$

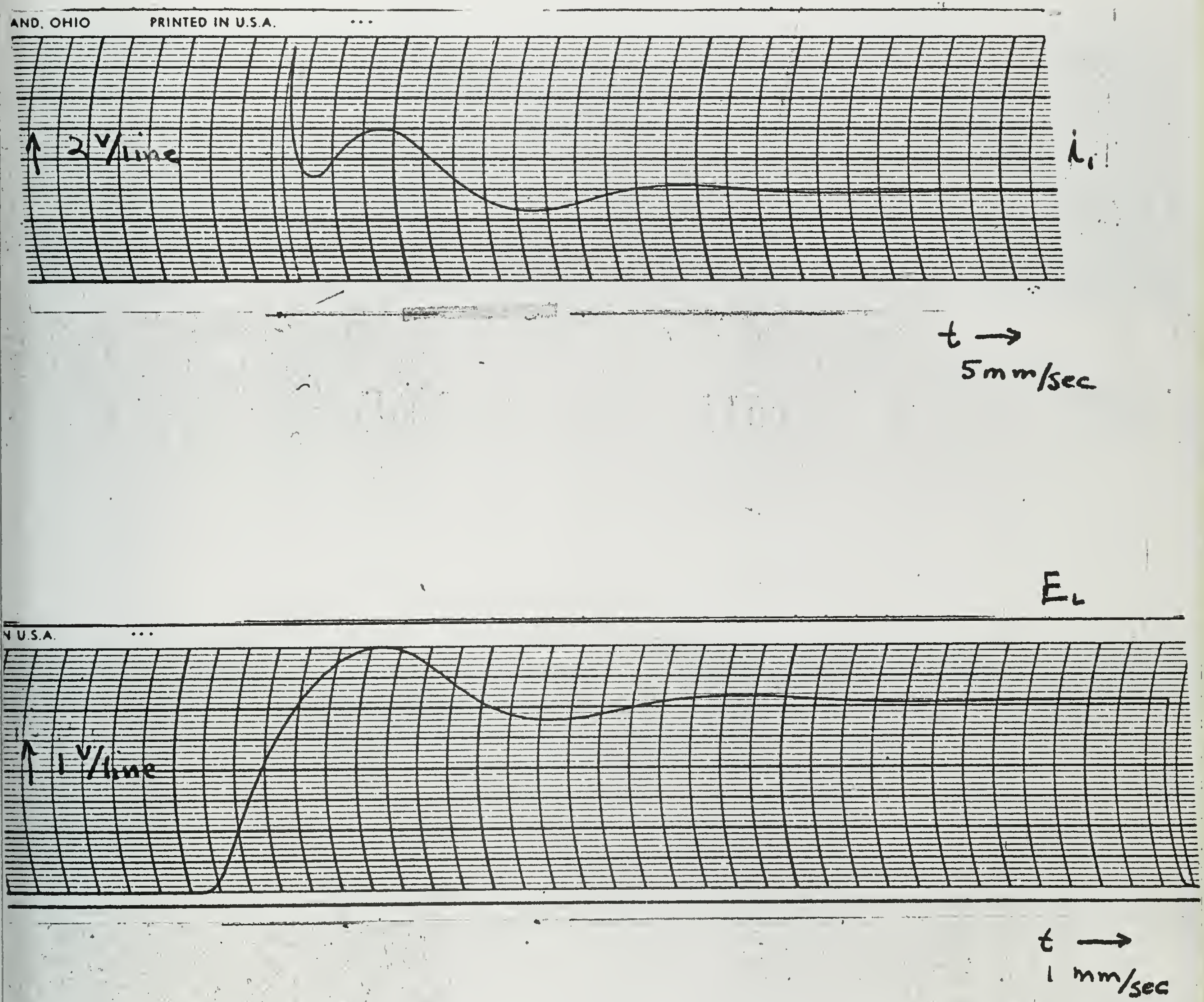

Fig. III-10

$C = 0.0212\ \mu f$ $\quad \xi = 0.302$

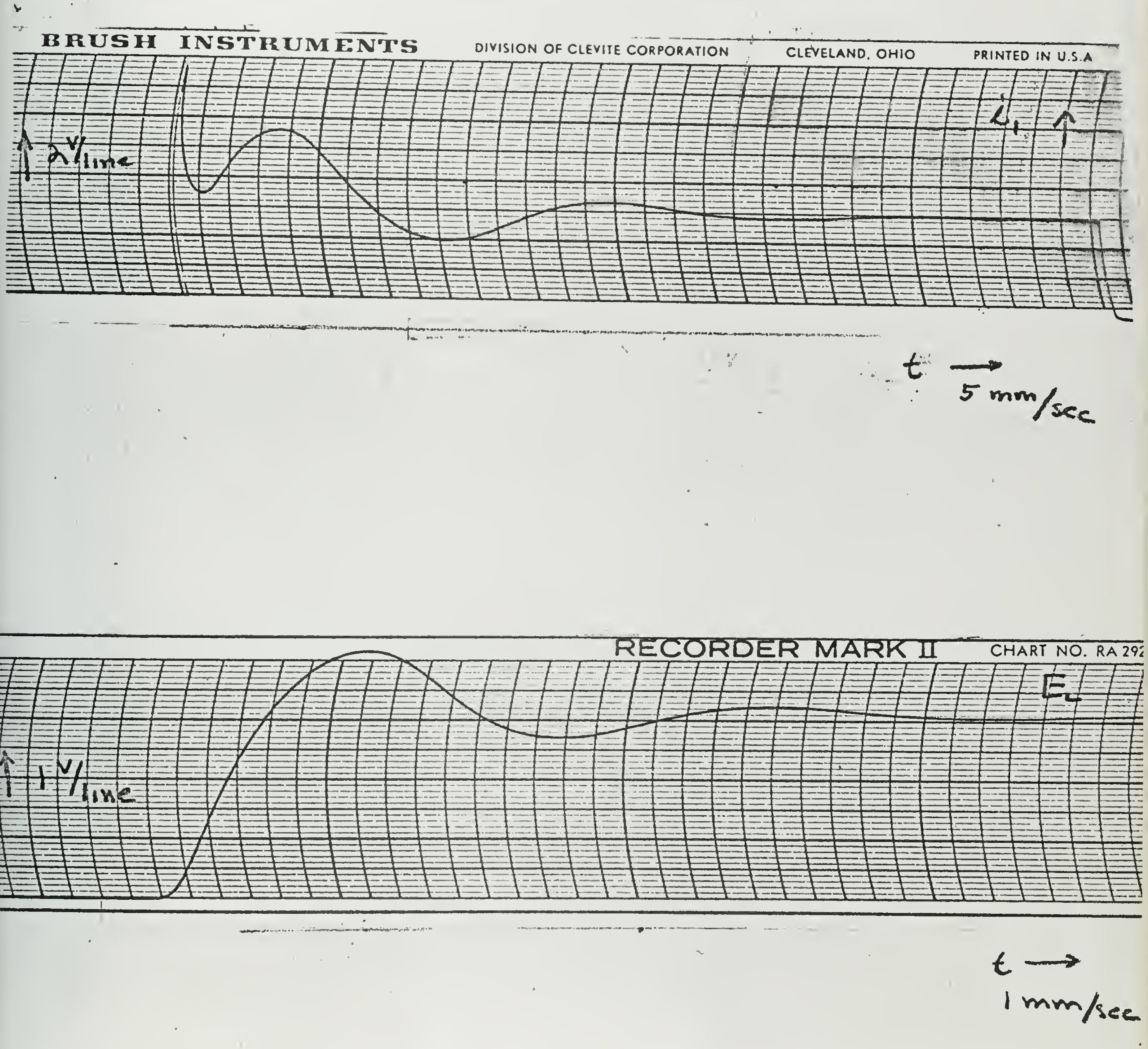

Fig. III-11

Figures III-12 through III-16 show what happens to the response when inductance is added. Additional inductance acts to dampen out the oscillations, however, there are limits to the amount of damping to be added, as is indicated by the slight lag in evidence in the current i_1 shown in Figure III-16. As more inductance is added we will be once more in danger of dropping below the rated holding current for the GICR with possible transformer saturation on the next half cycle.

The fixed parameters and scaling factors for Figures III-12 through III-16 are:

R_L = 1440 ohms

C = 0.00612 micro farads

α_i = 0.025

α_{E_L} = 6

$L = 9/8\ L_1$, $\alpha_t = 48 \times 10^4$

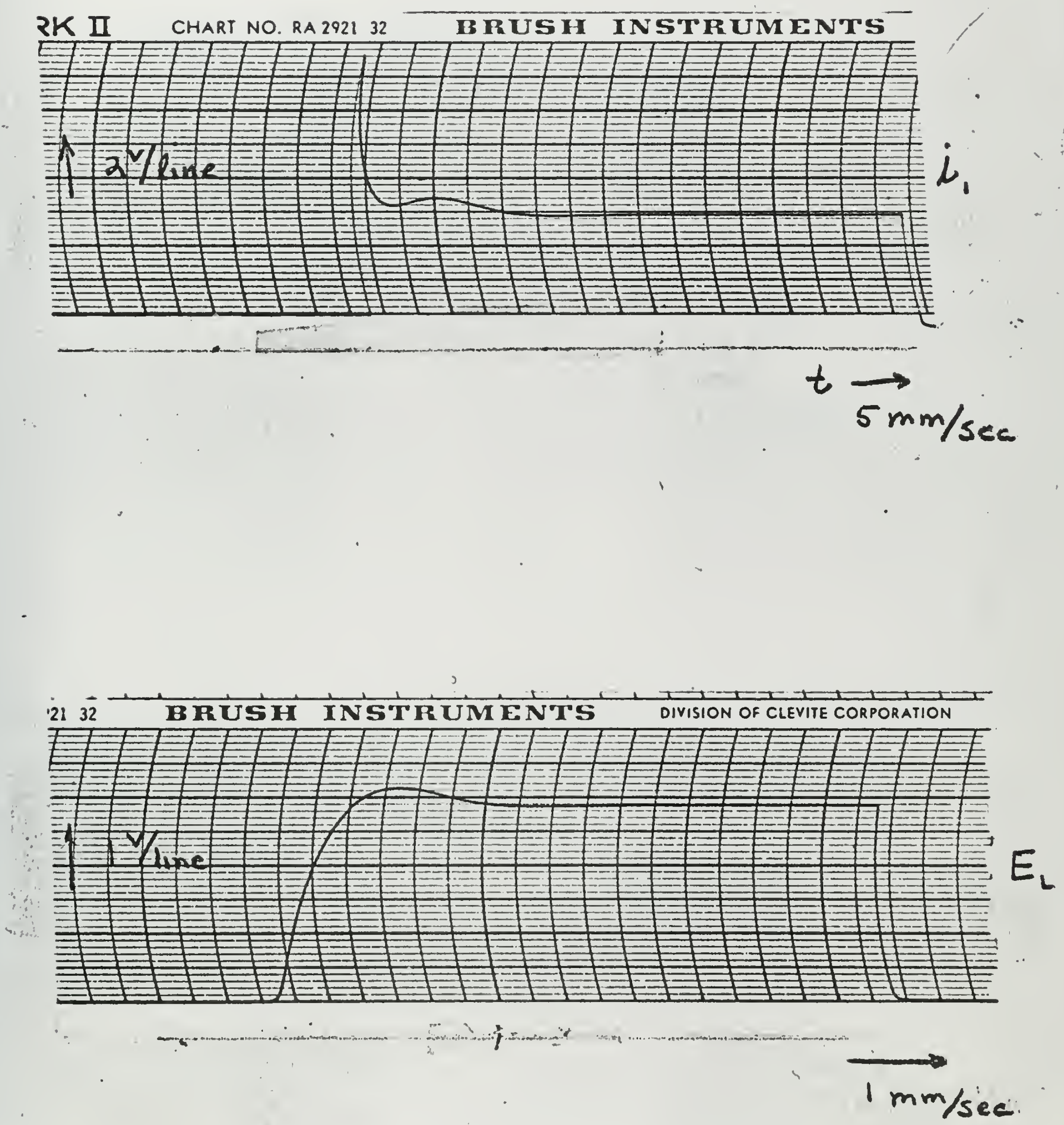

Fig. III-12

[illegible]

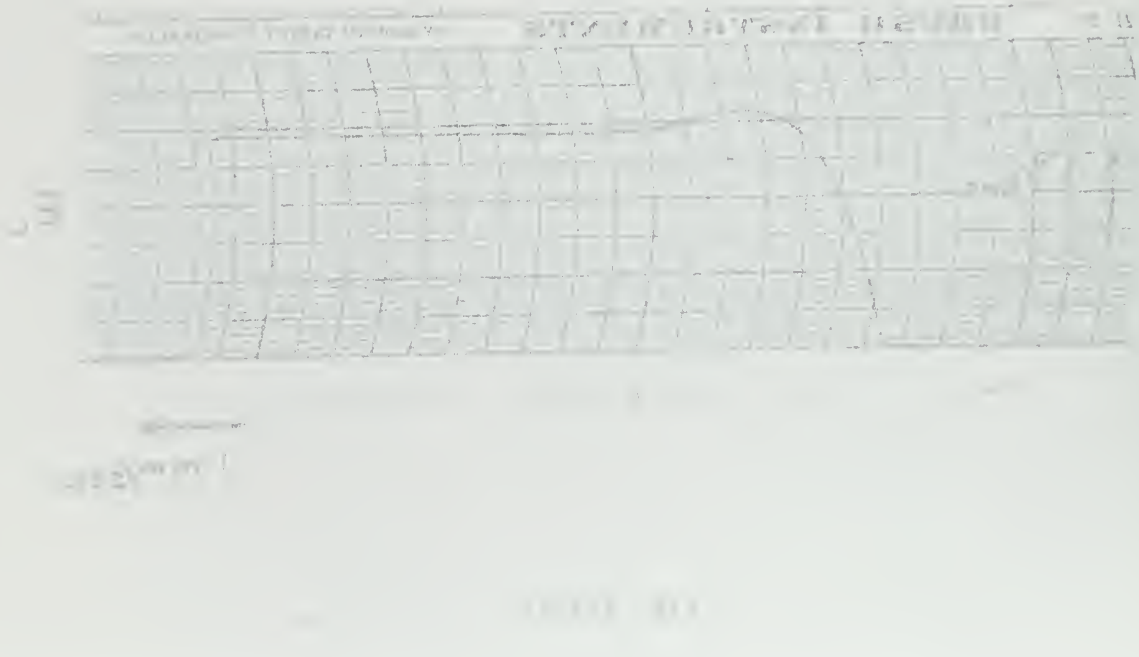

[illegible]

$L = 5/4\ L_1 \quad \alpha_t = 43.2 \times 10^4$

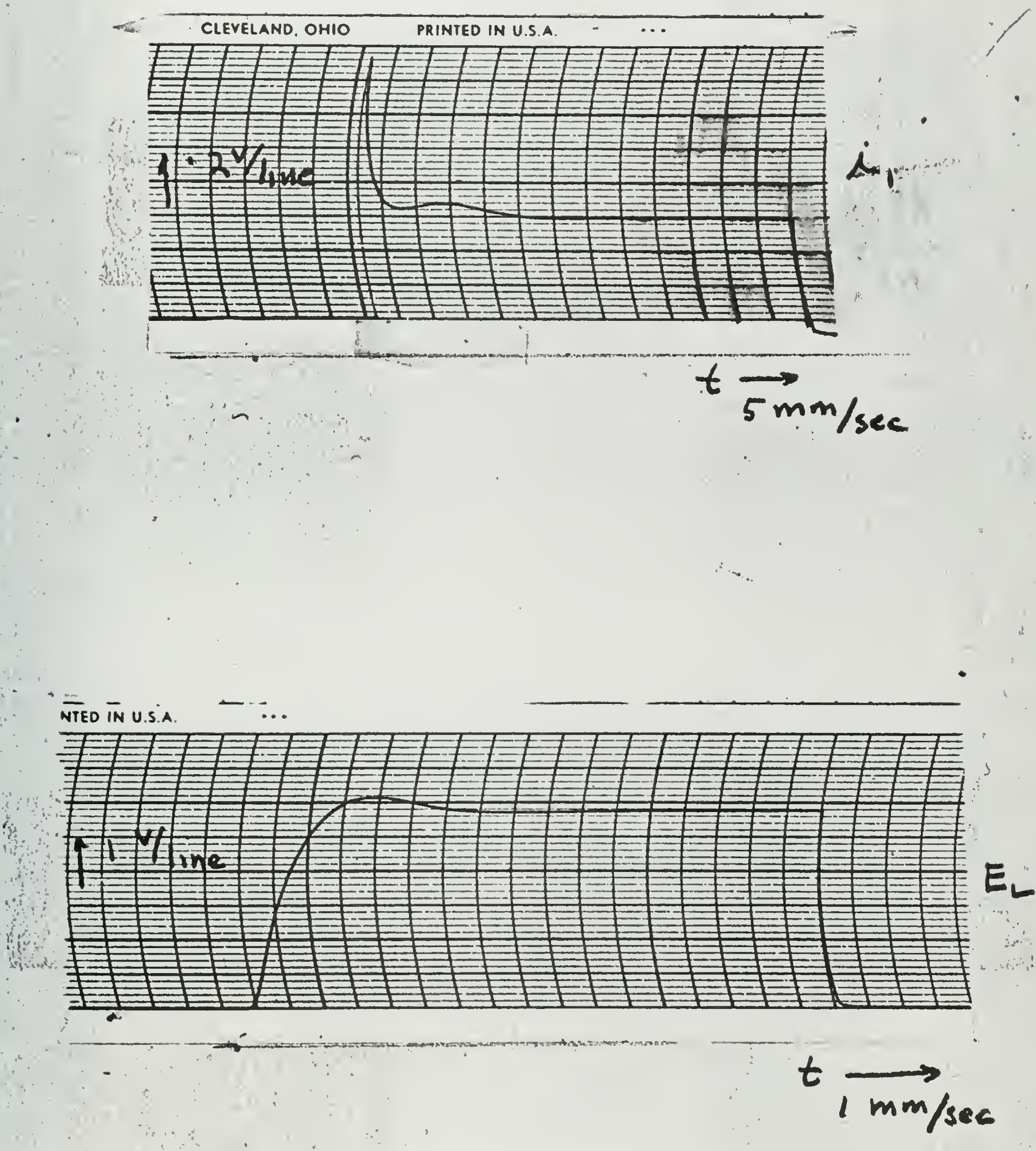

Fig. III-13

$L = 3/2\ L_1$ $= 36 \times 10^4$

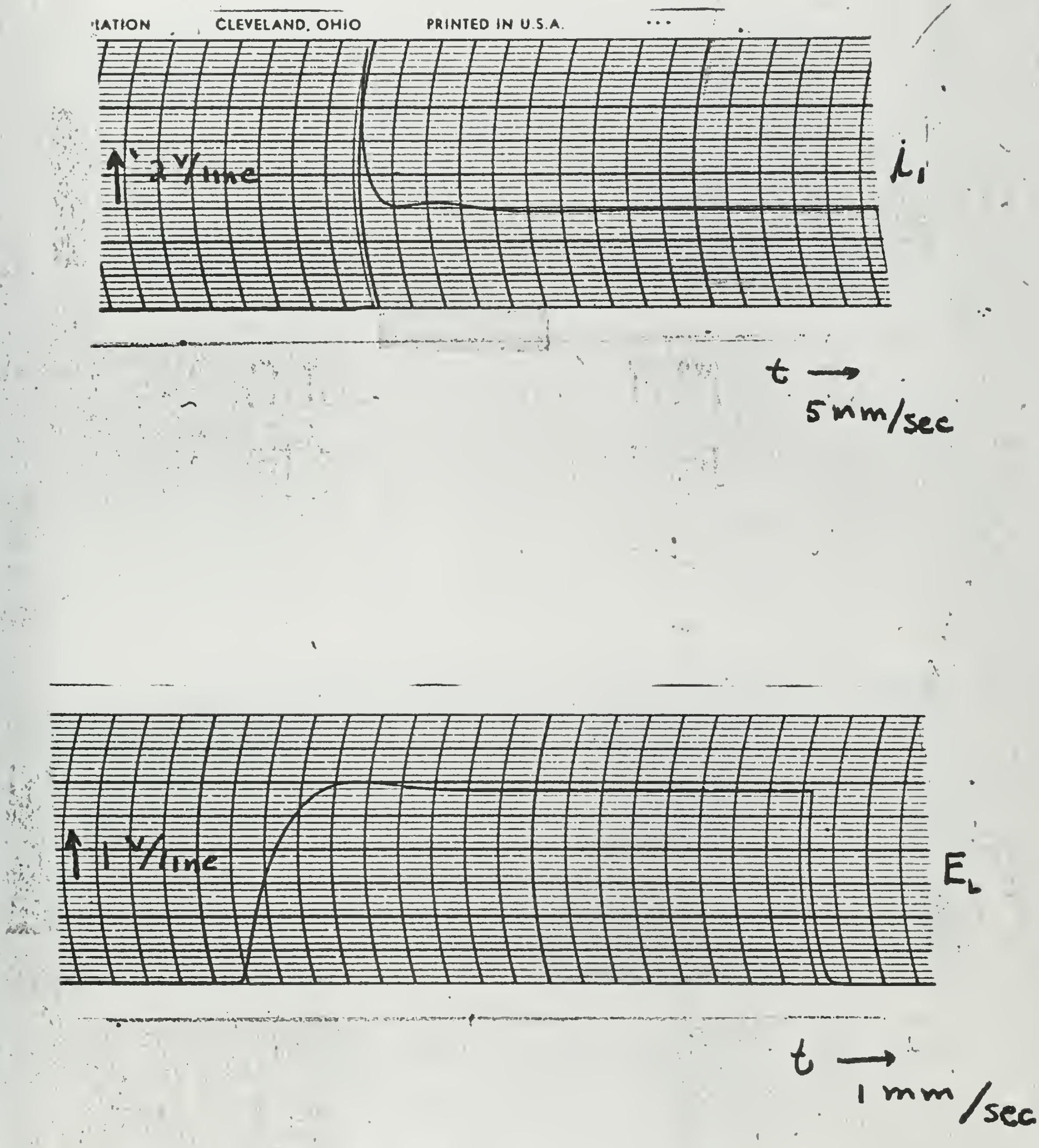

Fig. III-14

$L = 2 L_1 \qquad \alpha_t = 27 \times 10^4$

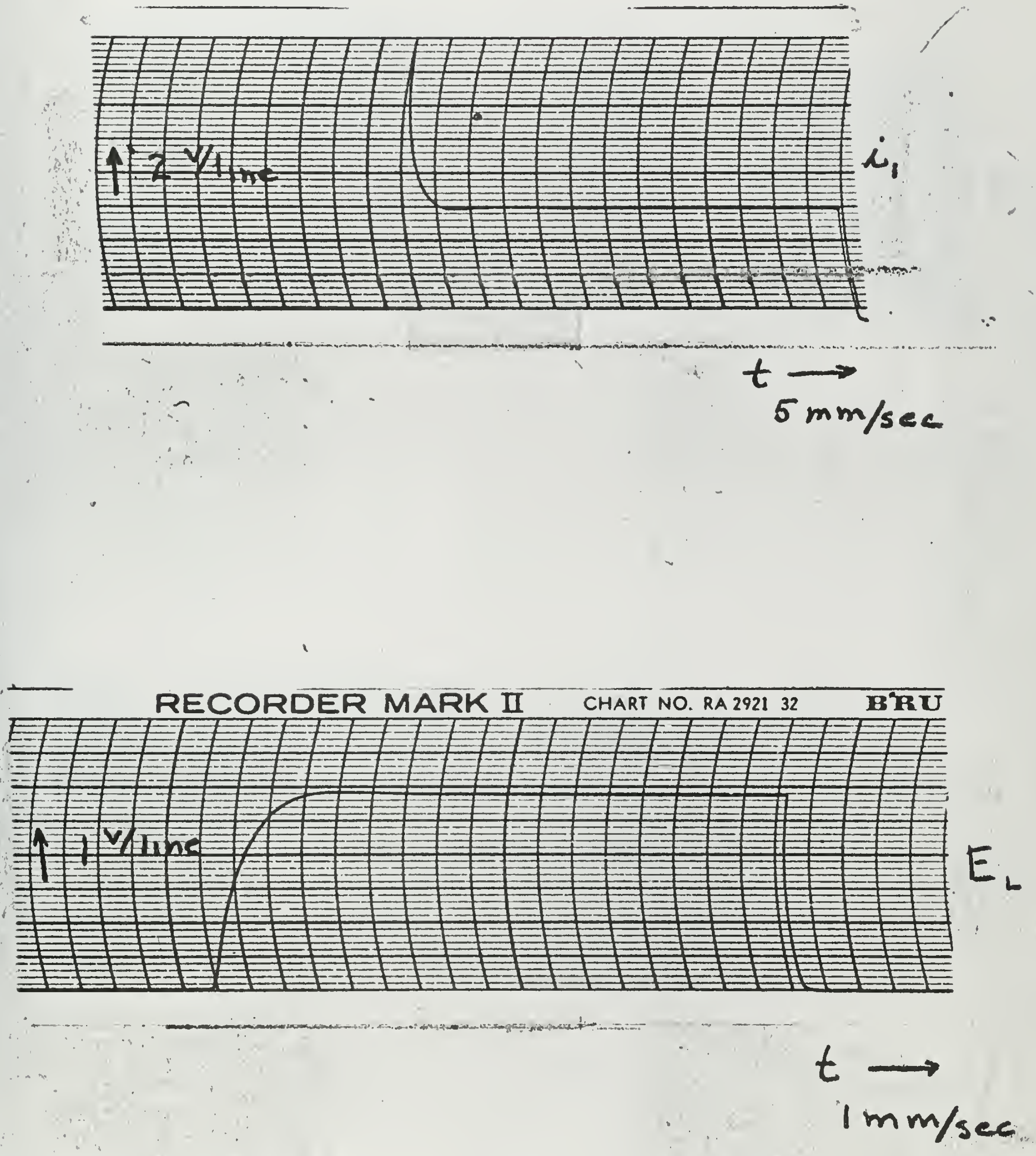

Fig. III-15

$L = 6\ L_1 \qquad \alpha_t = 9 \times 10^4$

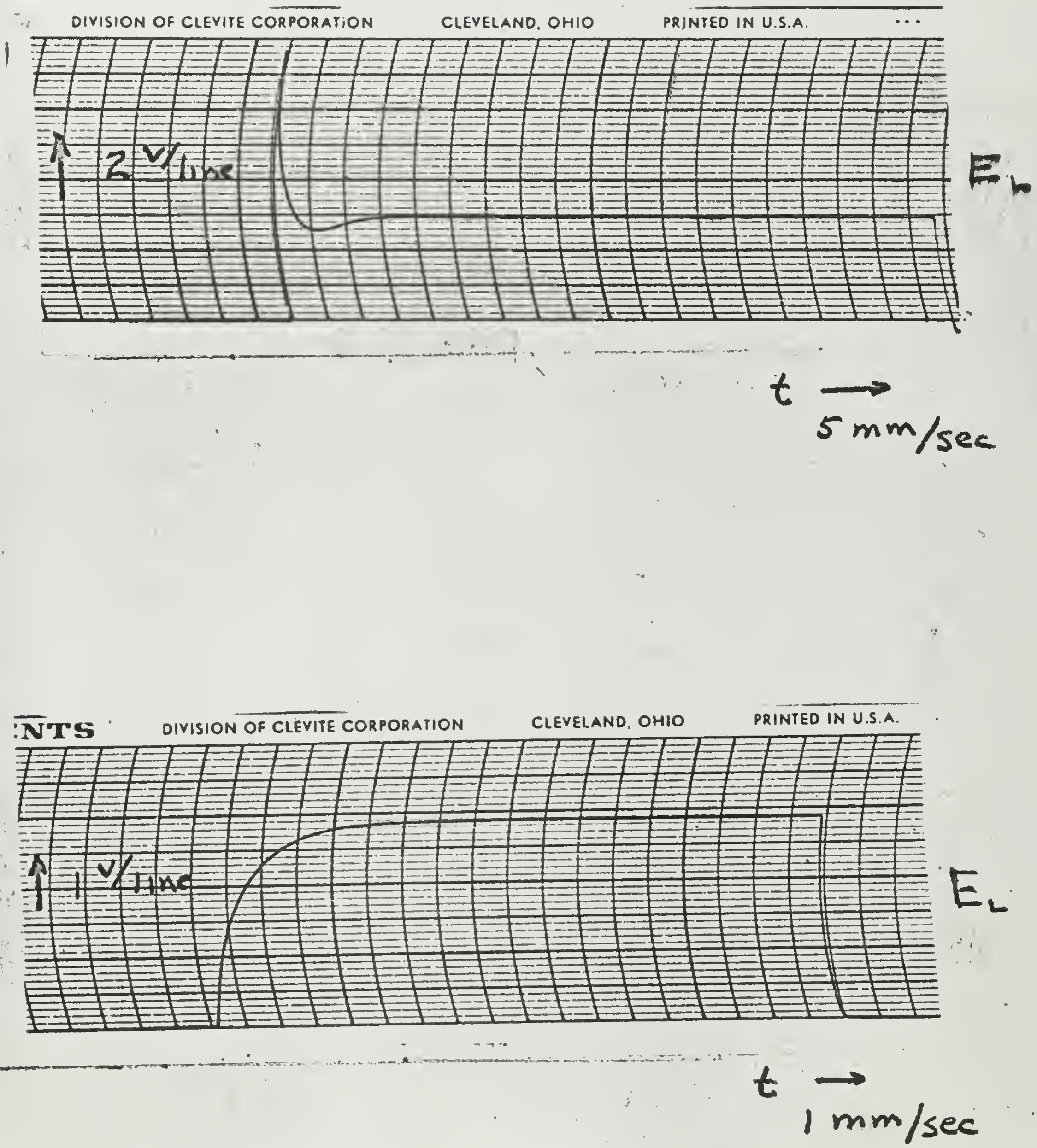

Fig. III-16

III.4 Experimental Results.

We can visually compare the predicted results with the observed values shown in Figures III-19 through III-25 and note about 1 to 6% deviation. Table A-1 portrays the tabulated experimental results and also shows the predicted values of overshoot based on the curve of Figure III-17.

TABLE A-1

C		M_{pt} cal	M_{pt} obs	% dev	Power gain	Efficiency
.0021	.95	1.008	1.064	5.27	1028	89%
.0042	.678	1.054	1.110	5.05		89%
.00612	.562	1.120	1.136	1.41		89%
.0082	.485	1.170	1.160	0.86		88%
.0110	.418	1.230	1.195	2.93		87.7%
.0160	.347	1.310	1.234	6.15		86.5%
.0212	.302	1.360	1.272	6.90		85.7%

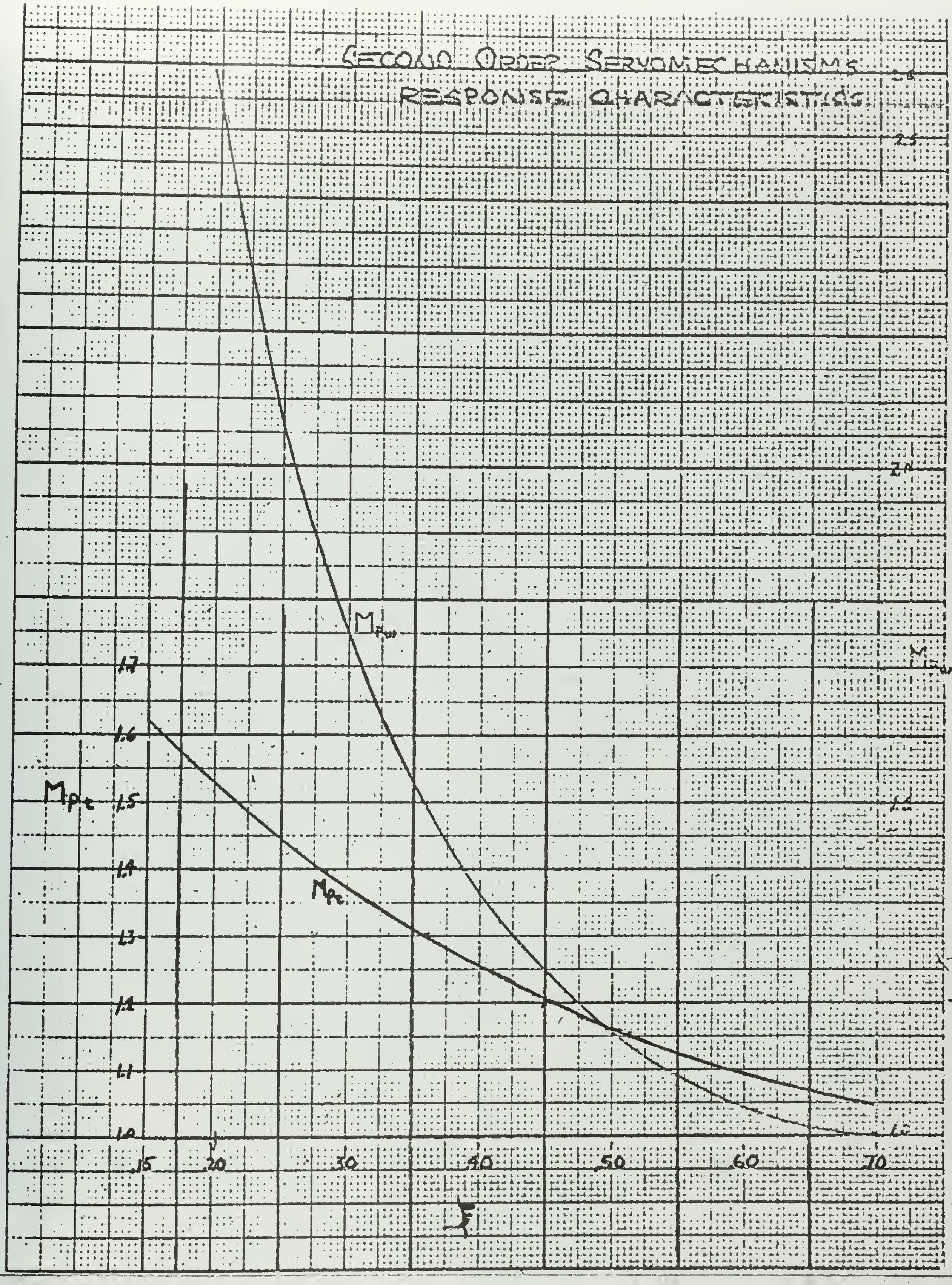
SECOND ORDER SERVOMECHANISMS
RESPONSE CHARACTERISTICS
2.5
2.0
M_pω
1.5
1.0
M_pω
M_pt
M_pt
1.7
1.6
1.5
1.4
1.3
1.2
1.1
1.0
.15
.20
.30
.40
.50
.60
.70
ζ

Fig. III-17

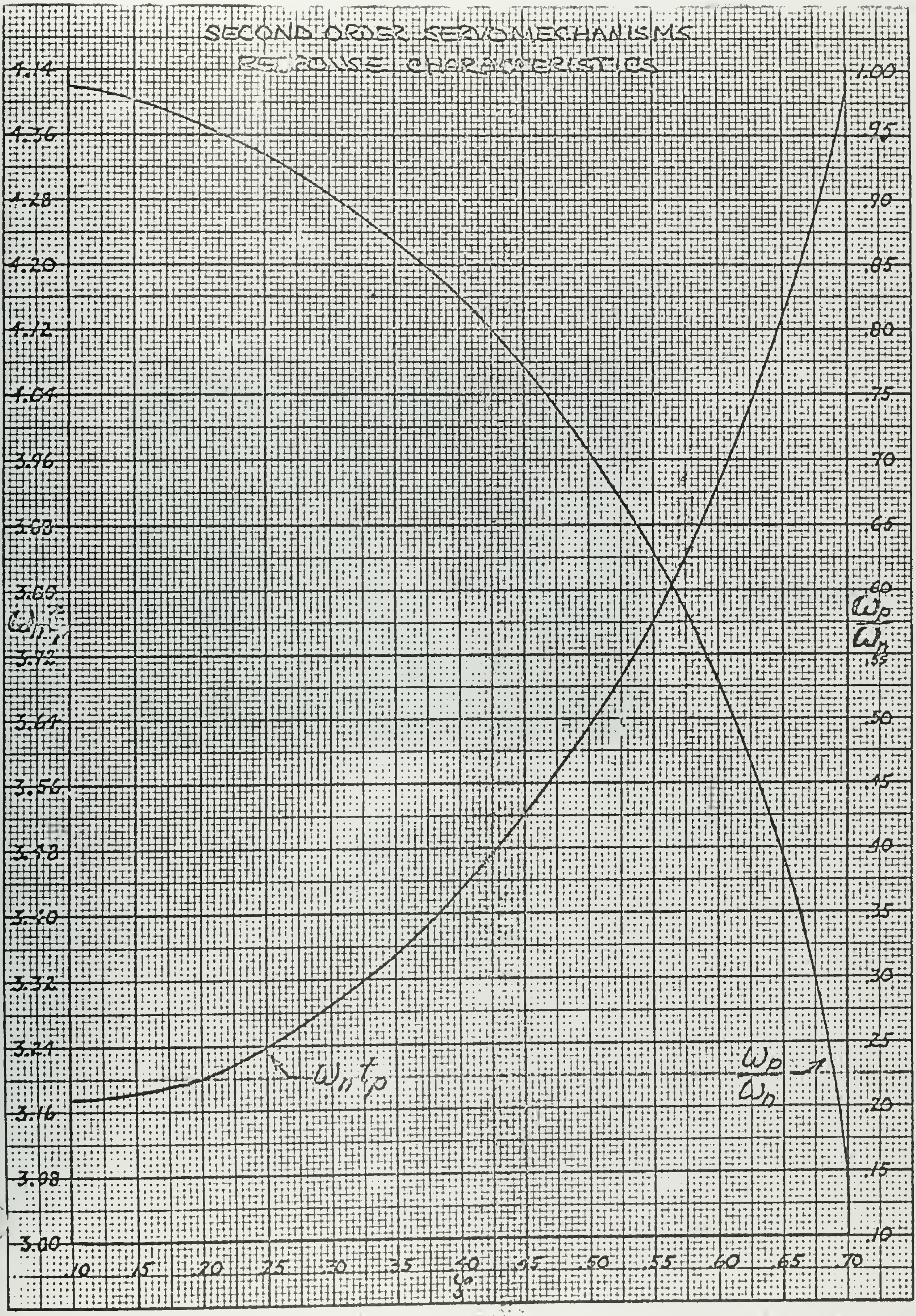
SECOND ORDER SERVOMECHANISMS
RESPONSE CHARACTERISTICS
4.44
4.36
4.28
4.20
4.12
4.04
3.96
3.88
3.80
3.72
3.64
3.56
3.48
3.40
3.32
3.24
3.16
3.08
3.00
$\omega_n t_p$
1.00
.95
.90
.85
.80
.75
.70
.65
.60
.55
.50
.45
.40
.35
.30
.25
.20
.15
.10
$\frac{\omega_p}{\omega_n}$
.10
.15
.20
.25
.30
.35
.40
.45
.50
.55
.60
.65
.70
ζ

Fig. III-18

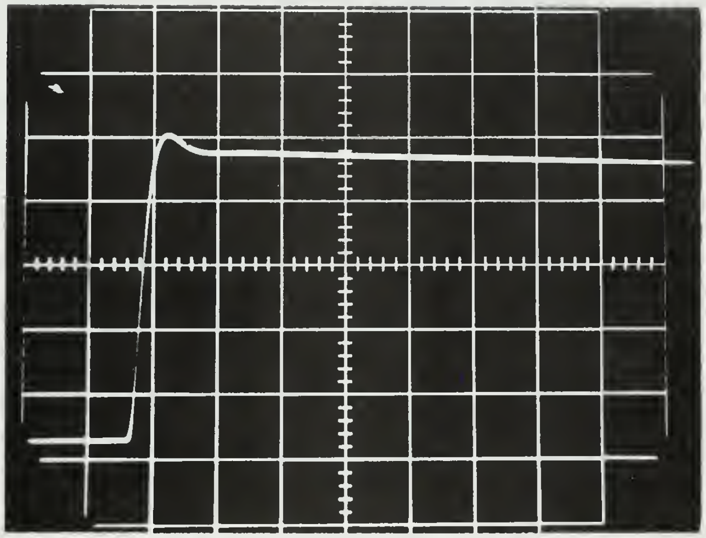

E_L
1 cm = 80 volts

time
1 cm = 40 μsec

Fig. III-19

Output Voltage E_L vs Time

C = .00212 μfarads

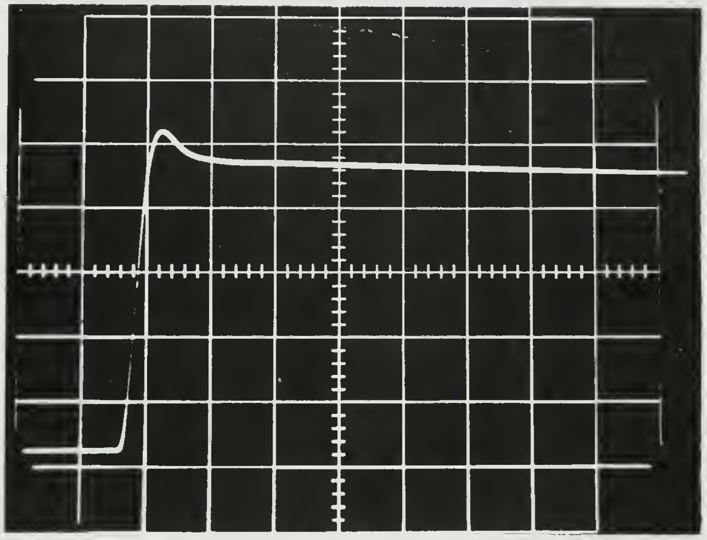

E_L

1 cm = 80 volts

time

1 cm = 40 μsec

Fig. III-20

Output Voltage E_L vs Time

C = .0042 μfarads

[illegible]

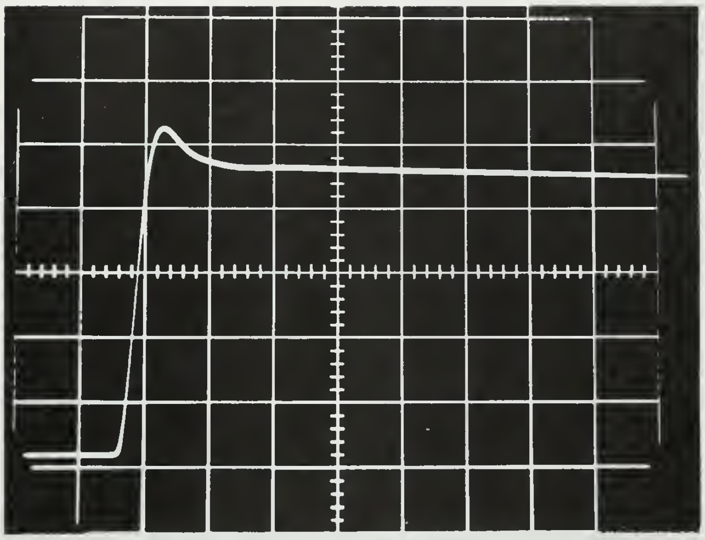

E_L

1 cm = 80 volts

time
1 cm = 40 μsec

Fig. III-21

Output Voltage E_L vs Time

C = .00612 μfarads

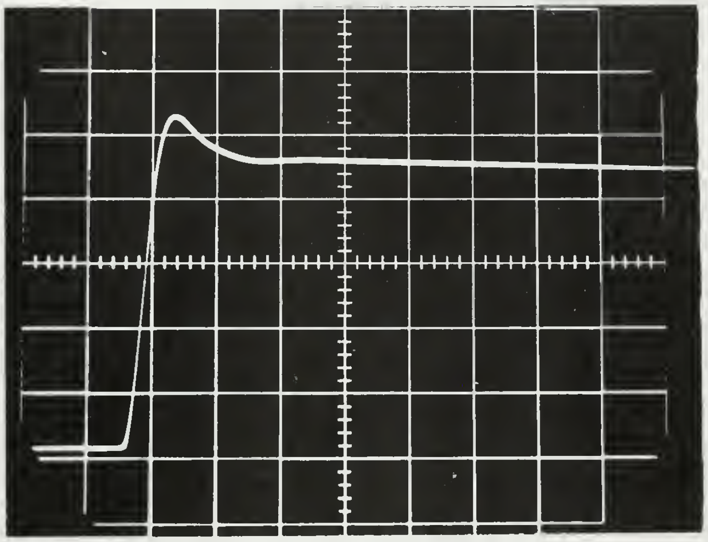

E_L

1 cm = 80 volts

time

1 cm = 40 μsec

Fig. III-22

Output Voltage E_L vs Time

C = .0082 μfarads

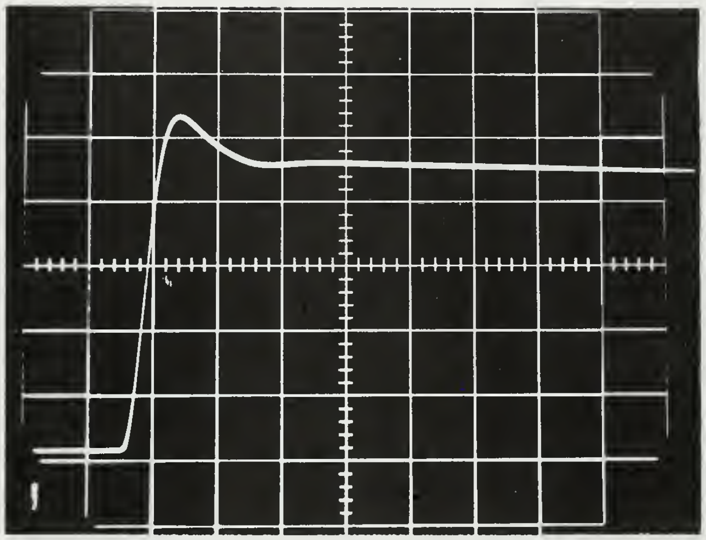

E_L

1 cm = 80 volts

time

1 cm = 40 μsec

Fig. III-23

Output Voltage E_L vs Time

C = .011 μfarads

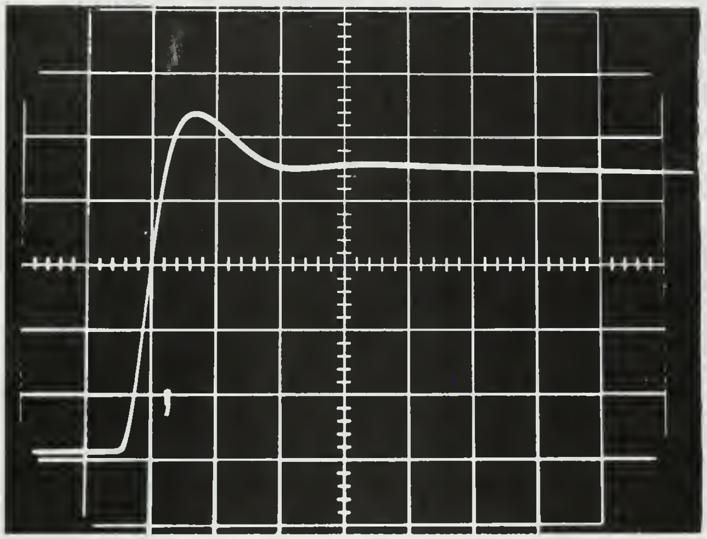

E_L

1 cm = 80 volts

time

1 cm = 40 μsec

Fig. III-24

Output Voltage E_L vs Time

C = .016 μfarads

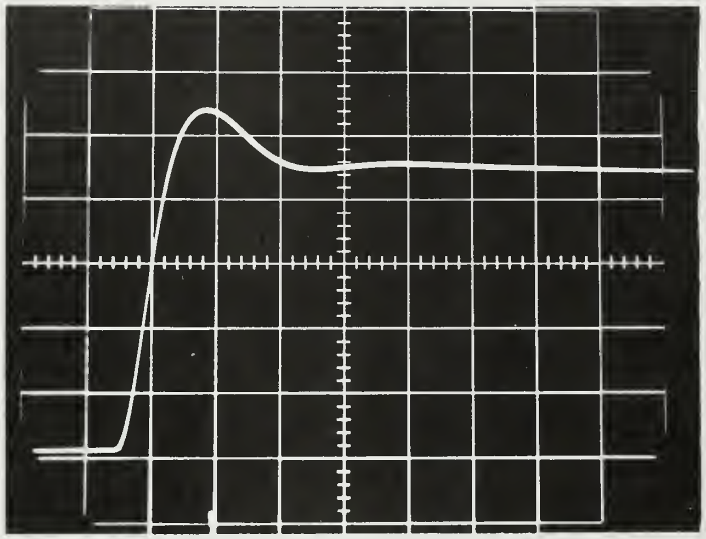

E$_L$
1 cm = 80 volts

time
1 cm = 40 μsec

Fig. III-25

Output Voltage E$_L$ vs Time

C = .021 μfarads

III.5 Conclusions Based on Experimental Results.

The basic reason for the observed deviation from predicted results is that the desired load could not be simulated with our laboratory components. The actual transfer functions were of third order rather than second order due to the inductance associated with the wire wound resistor used. Our actual load was really,

$$Z_L(s) = sL_L + \frac{R_L + sL_R}{s^2 L_R C + R_L C s + 1}$$

$$= L_L \left[\frac{S(S^2 + SR_L/L_R + 1/L_R C) + S/L_L C + R_L/L_R L_L C}{S^2 + R_L S/L_R + 1/L_R C} \right]$$

where L_R = the inductance due to the resistor.

The transfer function for output voltage was really:

$$\frac{E_1(s)}{E/N} = \frac{R_L + sL_R}{sL_L(s^2 L_R C + R_L C s + 1) + sL_R + R_L}$$

The system characteristic equation is then

$$s^3 + \frac{R_L s^2}{L_R} + \left(\frac{1}{L_R C} + \frac{1}{L_L C} \right) s + \frac{R_L}{L_R L_L C}$$

Letting

$$X(s) = s \left(\frac{1}{L_R C} + \frac{1}{L_L C} \right) + \frac{R_L}{L_R L_L C}$$

and

$$Y(s) = s^3 + \frac{R_L}{L_R} s^2$$

we can examine the effects of varying C by plotting x(s)/y(s) on a root locus plot and observing the movement of the roots.

$$\frac{X(S)}{Y(S)} = \frac{1}{L_R C} \quad \frac{\left(\frac{L_R + L_L}{R_L} \right) S + 1}{S^2 \left(\frac{L_R}{R_L} S + 1 \right)}$$

A sketch of the Root Locus plot for the actual experimental system is shown below

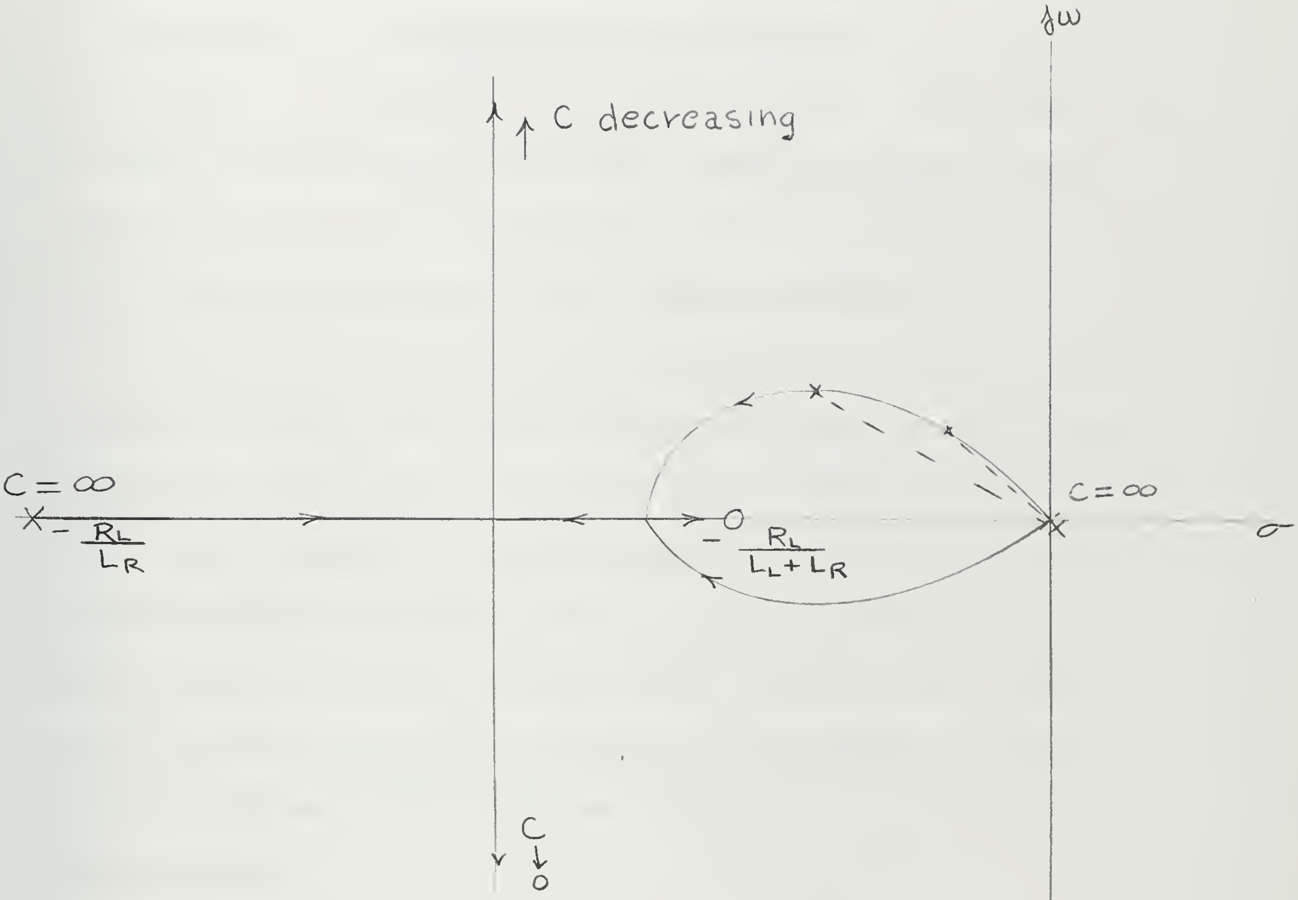

For the range of capacitance used in the laboratory, performance was approximately in the range shown by the dotted lines on the sketch.

In addition to the data tabulated, a dual beam oscilloscope was used to verify frequency correspondence. It was found that the leading edge of each pulse could be aligned with the zero crossings of the output voltage wave shape, hence frequency was preserved.

We can see now by examining both the analytical and observed results that for the range $\xi = .95$ to $\xi = .302$ the frequency has been preserved, the amplitude of the output voltage has deviated from the average half cycle value by at most 36%, and that efficiencies on the order of 85% at power gains of about 1000 are possible.

We could now predict that for this GTCR, rated at 400 volts and 2 amperes, we could, with a proper output transformer, operate safely at 200 watts output power with a power gain of 1000. The output transformer must be designed so that the reflected resistance allows rated current at the desired supply voltage, without saturating. Also, a resistor should be inserted during at least the first half cycle in series with the power supply to prevent the transformer from saturating due to residual flux of the same sense as the flux due to the inrushing current.

BIBLIOGRAPHY

1. Motto, J. W., Characteristics of the Gate Controlled Turn-Off Tranistor Controlled Rectifier. IEEE Conference Paper, IEEE Winter General Meeting, New York, New York. January 29, 1963. Paper No. CP 63-510.

2. Brunetto, Frank. Gate Turn-OFF Unique Solid State Switch. Electronics, April 26, 1963, 60-63.

3. Gentry, Finis E., Turn-On Criterion for p-n-p-n Devices. IEEE Transactions on Electron Devices. February 1964. p 74.

APPENDIX I

TRIGGERING CIRCUIT

The triggering circuit used in the experimental section is shown below:

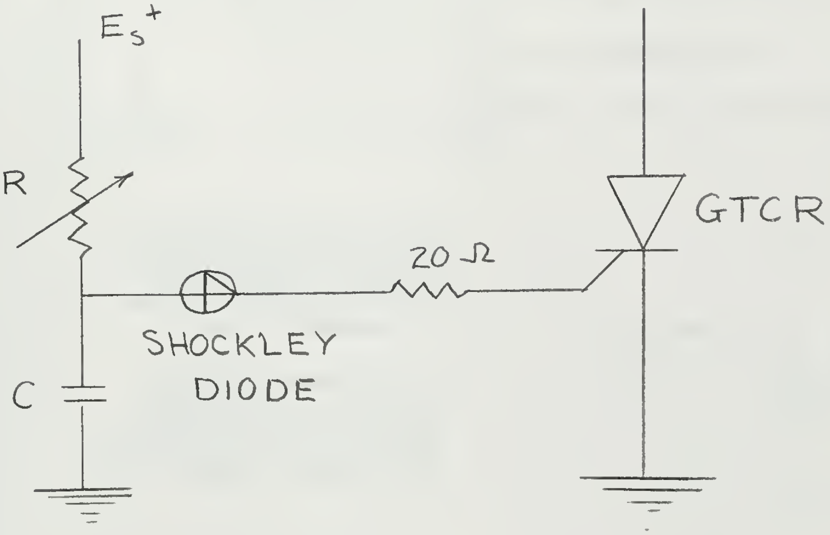

The Shockley diode is a four layer, Silicon, two terminal switch. The Voltage-Current characteristic curve for this p-n-p-n device shows two stable states, a high impedance state, Region I, and a low impedance state Region III. To turn the device on the voltage across the terminals must exceed the switching voltage, Vs. Turn-off is accomplished by reducing the current through the device below the rated holding current. The V-I curve and other diode characteristics are shown in Figure A-1.

For the triggering circuit, a Shockley diode with a switching voltage of 30 volts was used with the following effects on triggering operations:

1. Pulse Interval T

Characteristic V-I Curve

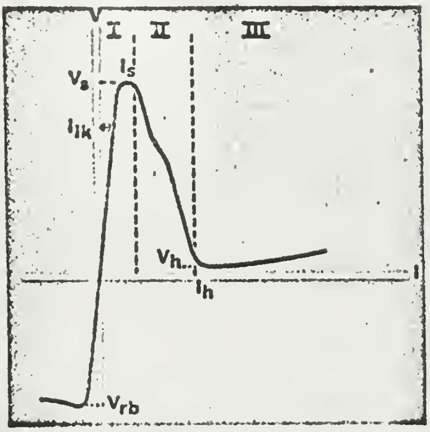

Terms and Symbols

V_s	Switching Voltage
I_s	Switching Current
I_h	Holding Current (or Sustaining Current)
V_h	Holding Voltage
R_{on}	"On" resistance (the slope of the V-I curve measured at currents $>I_h$)
I_{lk}	Leakage Current
V_{rb}	Reverse Breakover (Avalanche) Voltage

This is a diagram of the construction of the Shockley 4-layer diode. Produced from single-crystal silicon, the four layers are obtained by the controlled diffusion of suitable impurities.

The symbol for the Shockley 4-layer diode is a modified "4"; the slant line of the "4" indicates the forward direction of current passing through the device when in the "on" state.

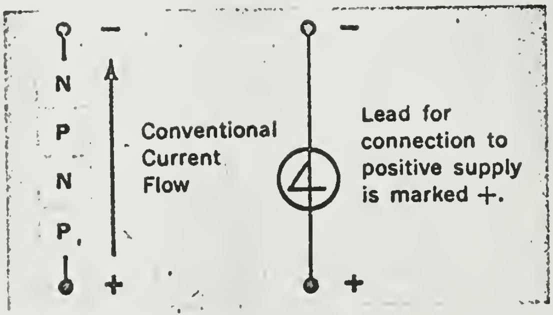

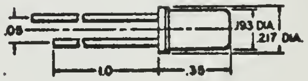

ERCIAL Series

D 4-LAYER DIODE FOR 2 AMPERE PULSE CURRENTS

e	Switching Voltage (V_s) in volts	Holding Current (I_h) in ma
-3	20 ± 4	1-6
-12	20 ± 4	5-20
-30	20 ± 4	19-45
-3	30 ± 4	1-6
-12	30 ± 4	5-20
-30	30 ± 4	19-45
-3	40 ± 4	1-6
-12	40 ± 4	5-20
-30	40 ± 4	19-45
-3	50 ± 4	1-6
-12	50 ± 4	5-20
-30	50 ± 4	19-45
-3	80 ± 8	1-6
-23	80 ± 8	5-45
0-3	120 ± 12	1-6
0-23	120 ± 12	5-45
0-3	200 ± 20	1-6
0-23	200 ± 20	5-45

Other Characteristics For All Standard Type D Units

Switching Current (I_s): $<125\mu a$

Holding Voltage (V_h): 0.5 to 1.2 volts

Current Carrying Capacity: 50 ma steady dc. Maximum peak current rating 2 amperes—dependent on duty factor, repetition rate, pulse duration and ambient temperature.

Turn-On Time: 0.1 μs (circuit will determine exact switching time)

Turn-Off Time: 0.2 μs (circuit will determine exact switching time)

Leakage Current (I_{lk}): $<15\ \mu a$ (measured at .75 V_s)

Dynamic Resistance On (R_{on}): <2 ohms at $I_h + 25$ ma and <0.3 ohm at 2 amperes

Capacitance: <100 pf (Exact value depends on V_s and applied voltage)

Ambient Temperature Operating Range: —40° to 65°C

Reverse Breakover (Avalanche) Voltage (V_{rb}): $>60\%$ of nominal switching voltage (V_s). Voltages applied in the reverse direction in excess of V_{rb} may cause damage to the device.

RATINGS ABOVE APPLY AT 25°C

Fig. A-1

We can calculate T by determining the time required to charge the capacitor to 30 volts. The expression for the voltage across the capacitor is

$$V_c = E_s \left(1 - \epsilon^{-\frac{t}{RC}} \right)$$

for Es = 100 volts, C = .1 μf and at time t = T,

Vc = 30.^{v}

hence

$$\frac{V_c}{E_s} - 1 = - \epsilon^{-\frac{t}{RC}}$$

$$\therefore\ t_1 = RC \ln\left(\frac{V_c}{E_s} - 1 \right) = .1\ R \ln\left(\frac{100}{70} \right) = .0358\ R\ \mu sec$$

2. Pulse height Ip

Ip = Vs/Rc = 30/20 = 1.5 amps

3. Pulse width t_w

The pulse width is the time required for the current to decay below the rated holding current of approximately 45 ma. Current decay can be expressed by,

$$I = Ip\ e^{-t/RcC}$$

which for the parameters used is

$$.045 = 1.5\ \epsilon^{-\frac{t_\omega}{2.0 \times 10^{6}}}$$

$$t_\omega = 2.0 \times 10^{-6} \ln\left(\frac{.045}{1.5} \right) = 7.6\ \mu \text{seconds}$$

APPENDIX II

ANALOG SOLUTION FOR AMPLIFIER CURRENT

The expression for amplifier current is,

$$I_1(s) = \frac{E}{N^2 R_L} \frac{R_L}{s(R_L C L_L s^2 + L_L s + R_L)} + \frac{E R_L C s}{N^2 R_L} \frac{R_L}{s(R_L C L_L s^2 + L_L s + R_L)} + \frac{2 E C_c}{s} \frac{s}{(R_c C_c s + 1}$$

using the variables as shown on the analog circuit diagram Figure A-2, the scaling equations become:

Let $\overset{\llcorner}{F} = F(s)$,

$$\overset{\llcorner}{E}_i = \frac{\alpha_E}{\alpha_{E_i}} \frac{\overset{\llcorner}{E}}{R_L N^2}$$

$$\alpha_E = 1 \qquad \alpha_{E_i} = \frac{1}{N^2 R_L}$$

$$R_1 = R_{f1} = 1 \text{ Meg-ohm}$$

$$a_1 = 1$$

$$\overset{\llcorner}{\mathcal{E}} = \frac{\alpha_{E_i}}{\alpha_{\mathcal{E}}} \overset{\llcorner}{E}_i - \frac{\alpha_{i_1'}}{\alpha_{\mathcal{E}}} \overset{\llcorner}{I}_1'$$

$$\alpha_{\mathcal{E}} = \alpha_{E_i} = \alpha_{i_1'}$$

$$R_2 = R_3 = R_{f3} = 1 \text{ Meg-ohm}$$

$$a_2 = a_3 = 1$$

$$\overset{\llcorner}{\dot{I}}_1' = \frac{\alpha_{\mathcal{E}}}{\alpha_{\dot{i}_1'}} \frac{R_L}{L_L} \overset{\llcorner}{\mathcal{E}} \frac{1}{(RCs+1)}$$

$$\alpha_{\dot{i}_1'} = \frac{1}{N^2 L_L} \qquad \alpha_t = \frac{R_L}{L_L} = 9 \times 10^4$$

$L_L = .016$ henries
$R_L = 1440\ \Omega$

$$\frac{a_4 R_{f4}}{a_6 R_6} = 1$$

$$\frac{C_{f4} R_{f4}}{a_6} = \frac{R_L^2 C}{L_L} = 129.6\, C \times 10^6$$

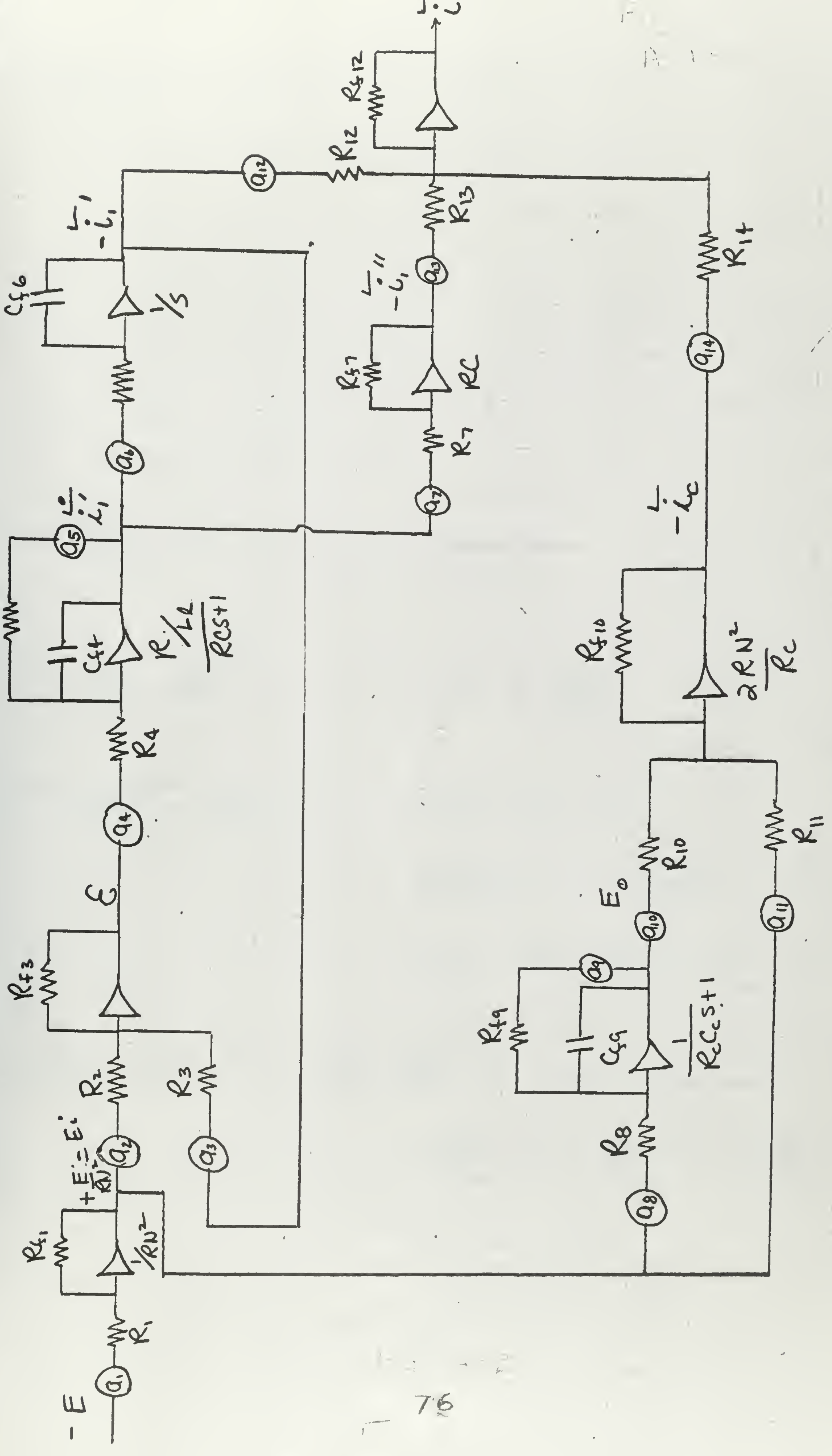
$-E$
a_1
R_1
R_{f1}
$1/RN^2$
$+\frac{E}{(RN)^2} = E_i$
a_2
R_2
R_3
a_3
R_{f3}
ε
a_4
R_4
R_{f4}
C_{f4}
$\frac{R/L_2}{RCs+1}$
a_5
$\dot{i}_1$
a_6
C_{f6}
$1/s$
$-i_1'$
a_{12}
R_{12}
R_{f12}
i_1
R_{13}
a_{13}
$-i_1''$
R_{f7}
RC
R_7
a_7
R_{14}
a_{14}
$-i_c$
R_{f10}
$\frac{2RN^2}{R_c}$
R_{10}
R_{11}
E_0
a_{10}
a_{11}
a_9
R_{f9}
C_{f9}
$\frac{1}{R_cC_cs+1}$
R_8
a_8

In Tabular Form the, for R_L and L_c fixed and C variable.

C μf	a_6	C_{f4} μf	R_{f4} MΩ	R_9	a_4
.0021	.919	1	.25	.25	.919
.0042	.46	1	.25	.25	.46
.00612	.315	1	.25	.25	.315
.0082	.94	1	1	1	.94
.011	.702	1	1	1	.702
.016	.483	1	1	1	.483
.0212	.364	1	1	1	.364

$$\bar{I}_1' = \int \frac{\alpha_{\dot{\bar{i}}_1'}}{\alpha_{i_1'}\alpha_t} \dot{\bar{I}}_1' \, dt$$

$$\frac{a_5}{R_5 C_{f5}} = 1 \qquad a_5 = 1$$

$R_5 = 1$ MΩ

$C_{f5} = 1$ μf

$$\bar{I}_1'' = \frac{\alpha_{\dot{\bar{i}}_1'}}{\alpha_{i_1''}} R_L C \dot{\bar{I}}_1'$$

$$\alpha_{i_1''} = \frac{R_L C}{N^2 L_L} \qquad a_7 = 1$$

$R_7 = R_{f7} = 1$ MΩ

$$\bar{E}_o = \frac{\alpha_{E_i}}{\alpha_{E_o}} \bar{E}_i \frac{1}{R_c C_c s + 1}$$

$$\alpha_{E_o} = \alpha_{E_i} = \frac{1}{N^2 R_L}$$

$$\frac{a_8 R_{f8}}{a_9 R_8} = 1 \qquad \frac{C_{f8} R_{f8}}{a_9} = R_c C_c \alpha_t$$

$$= .405$$

$C_{f8} = 1$ μf $\quad R_8 = R_{f8} = .25$ MΩ

$$a_8 = a_9 = .617$$

$$\bar{I}_c = \frac{\alpha_{E_i}}{\alpha_{i_c}} \frac{2 R_L N^2}{R_c} \bar{E}_i - \frac{\alpha_{E_o}}{\alpha_{i_c}} \frac{2 R_L N^2}{R_c} \bar{E}_o \qquad \alpha_{i_c} = \alpha_{E_o} = \alpha_{E_i}$$

$$a_{10} \frac{R_{f10}}{R_{10}} = a_{11} \frac{R_{f10}}{R_{11}} = \frac{2 R_L N^2}{R_c}$$

$R_{f10} = 1$ MΩ $\quad R_{10} = R_{11} = .25$ MΩ

$$a_{10} = a_{11} = .667$$

$$\bar{I}_1 = \frac{\alpha_{i_1}'}{\alpha_{i_1}} \bar{I}_1' + \frac{\alpha_{i}''}{\alpha_{i_1}} \bar{I}_1'' + \frac{\alpha_{ic}}{\alpha_{i_1}} \bar{I}_c \qquad \alpha_{\mu_1} = \alpha_{i_1}' = \alpha_{\mu c} = \frac{1}{N^2 R_L}$$

$$R_{f12} = R_{12} = R_{14} = 1 \ M\Omega$$

$$a_{12} = a_{14} = 1$$

$$a_{13} = R_L C \alpha_t \left(\frac{R_{13}}{R_{f12}} \right)$$

$$= 129.6 \times 10^6 \ C \ \frac{R_{13}}{R_{f12}}$$

for $R_{13} = .1 \ M\Omega$

C μf	a_{13}
.0021	.0272
.0042	.0544
.00612	.0793
.0082	.0162
.011	.1425
.016	.207
.0212	.2745

Now keeping R_L = 1440 Ω and C fixed at .00612 μf vary L in steps as follows:

$$L = \frac{9}{8} L_L, \ \frac{5}{4} L_L, \ \frac{3}{2} L_L, \ 2 L_L, \ 6 L_L$$

The only modifications to the above occur due to change in $\alpha_t = \frac{R_L}{L_L}$. Hence affected pots are varied a_4 and a_6 increasing and a_{13} decreasing.

L	a_4'	a_6'	a_{13}'	
9/8 L_1	.3545	.3545	.0705	
5/1 L_1	.394	.394	.0635	
3/2 L_1	.473	.473	.053	
2 L_1	.709	.709	.0353	
6 L_c	.756	.756	.0112	with $R_{f4} = R_4 = .1\ M\Omega$

APPENDIX III

ANALOG SOLUTION FOR OUTPUT VOLTAGE

Next write the equation for output voltage

$$\bar{E}_L = \frac{E}{N} \quad \frac{R_L}{s(R_L C L_L s^2 + L_L s + R_L)}$$

which in transfer function form is:

$$\frac{\bar{E}_L}{\bar{E}/N} = \frac{R_L}{R_L C L_L S^2 + L_L S + R_L}$$

For analog simulation consider then that

$$\frac{R_L}{R_L C L_L S^2 + L_L S + R_L} = \frac{F_o}{1 + F_o}$$

where $F_o = \dfrac{R_L/L_L}{s(R_L C s + 1)}$ which becomes

the open loop transfer function in the feedback analog circuit shown in Fig. A-3. The analog expressions are then:

$$\frac{\bar{E}}{N} = \frac{\alpha_{\dot{o}}}{\alpha_E} 100 \qquad a_1 = .3 \qquad R_1 = R_{f1} = 1 \text{ M}\Omega$$

$$\bar{\varepsilon} = \frac{\alpha_E}{\alpha_\varepsilon} \frac{\bar{E}}{N} - \frac{\alpha_{EL}}{\alpha_\varepsilon} \bar{E}_L \qquad \alpha_\varepsilon = \alpha_E = \alpha_{EL} = 6$$

$$a_2 = a_3 = 1 \qquad R_2 = R_3 = R_{f2} = 1 \text{ M}\Omega$$

$$\dot{\bar{E}}_L = \frac{\alpha_\varepsilon}{\alpha_{\dot{E}L}} \varepsilon \frac{R_L/L_L}{R_L C s + 1} \qquad \alpha_t = 6 \frac{R_L}{L_L} = 54 \times 10^4$$

$$\frac{R_{f4} C_{f4}}{a_5} = R_L C \alpha_t$$

$$a_5 = \frac{R_{f4} C_{f4}}{R_L C \alpha_t} \qquad a_4 = a_5 \frac{R_4}{R_{f4}}$$

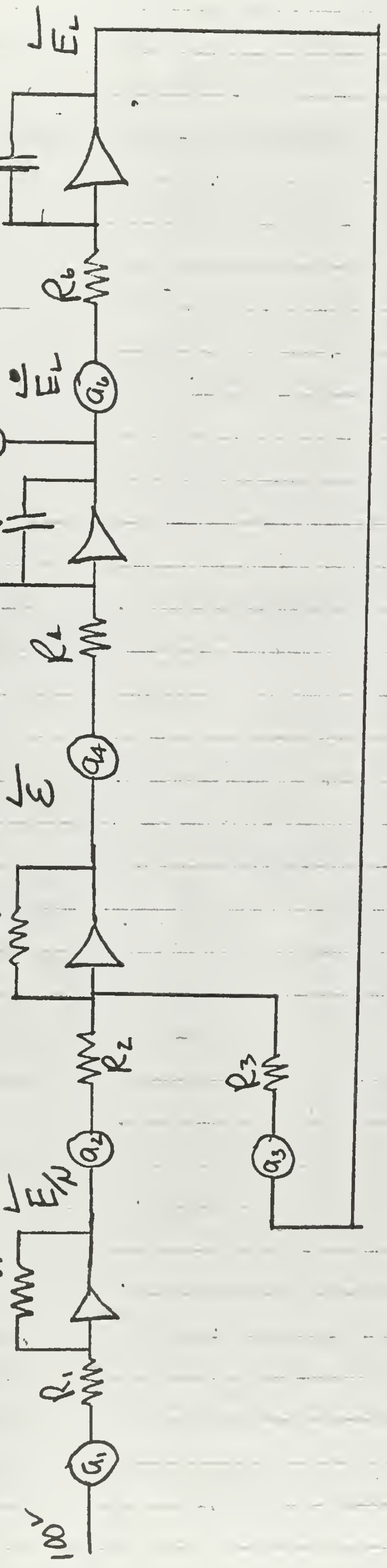

Fig. A-3

First let $R = 1440\,\Omega$ and $L_L = .016$ h remain fixed and vary C. The pot settings for a_4 and a_5 may be tabulated as shown below:

C μf	C_4 μf	R_{f4} MΩ	R_4	a_5	a_4
.0021	1	1	1	.603	.603
.0042	1	1	1	.3015	.3015
.00612	1	1	1	.210	.210
.0082	1	1	1	.157	.157
.011	1	1	1	.117	.117
.016	1	1	1	.0804	.0804
.0212	1	1	1	.0606	.0606

$$\bar{E}_L = \int \frac{\alpha_{\dot{E}_L}}{\alpha_{E_L}\alpha_t} \dot{\bar{E}}_L \, dt \qquad \frac{a_6}{R_6 C_{f6}} = \frac{1}{6}$$

$R_6 = 1\ \mathrm{M}\Omega$

$C_{f6} = 1\ \mu f$

$a_6 = .167$

Now keep $R = 1440\,\Omega$, $C = .00612\ \mu f$ and vary L_1. The required changes will be in pot settings a_4 and a_5.

L	a_5	a_4	α_t
$9/8\ L_1$	.236	.236	48×10^4
$5/4\ L_1$	.2625	.2625	43.2×10^4
$3/2\ L_1$	.315	.315	36×10^4
$2\ L_1$	.42	.42	27×10^4
$6\ L_1$	.315	.315	9×10^4 (change $R_{f4} = R_4 = .25\ \mathrm{M}\Omega$)

thesC192
Power amplification with gate turn-off c
3 2768 001 01985 4
DUDLEY KNOX LIBRARY